Article

SOURCE DATA | TRANSPARENT PROCESS

THE EMBO JOURNAL

TSC2 regulates tumor susceptibility to TRAIL-mediated T-cell killing by orchestrating mTOR signaling

Chun-Pu Lin[1], Joleen J H Traets[1,2], David W Vredevoogd[1], Nils L Visser[1] & Daniel S Peeper[1,*]

Abstract

Resistance to cancer immunotherapy continues to impair common clinical benefit. Here, we use whole-genome CRISPR-Cas9 knockout data to uncover an important role for Tuberous Sclerosis Complex 2 (TSC2) in determining tumor susceptibility to cytotoxic T lymphocyte (CTL) killing in human melanoma cells. TSC2-depleted tumor cells had disrupted mTOR regulation following CTL attack, which was associated with enhanced cell death. Wild-type tumor cells adapted to CTL attack by shifting their mTOR signaling balance toward increased mTORC2 activity, circumventing apoptosis, and necroptosis. TSC2 ablation strongly augmented tumor cell sensitivity to CTL attack *in vitro* and *in vivo*, suggesting one of its functions is to critically protect tumor cells. Mechanistically, TSC2 inactivation caused elevation of TRAIL receptor expression, cooperating with mTORC1-S6 signaling to induce tumor cell death. Clinically, we found a negative correlation between TSC2 expression and TRAIL signaling in TCGA patient cohorts. Moreover, a lower TSC2 immune response signature was observed in melanomas from patients responding to immune checkpoint blockade. Our study uncovers a pivotal role for TSC2 in the cancer immune response by governing crosstalk between TSC2-mTOR and TRAIL signaling, aiding future therapeutic exploration of this pathway in immuno-oncology.

Keywords mTOR; T-cell sensitivity; TRAIL; TSC2; tumor cells
Subject Categories Cancer; Immunology; Molecular Biology of Disease
DOI 10.15252/embj.2022111614 | Received 8 May 2022 | Revised 8 December 2022 | Accepted 14 December 2022 | Published online 30 January 2023
The EMBO Journal (2023) 42: e111614

Introduction

Immunotherapy, particularly immune checkpoint blockade (ICB), has transformed cancer patient care in recent years. The blockade of inhibitory immune checkpoints, such as programmed cell death 1 (PD-1) and cytotoxic T lymphocyte-associated protein 4 (CTLA-4), unleashes a potent antitumor response with cytotoxic T cells (CTLs) for a growing number of patients (Hodi *et al*, 2010; Larkin *et al*, 2015, 2019; Schadendorf *et al*, 2017; Wolchok *et al*, 2017).

Cytotoxic T cells are activated when their T-cell receptors (TCRs) encounter matching antigens presented by antigen-presenting cells (APC) or tumor cells. This can result in the elimination of target cells by the secretion of cytotoxic molecules, death ligands, and cytokines triggering cell death signaling (Russell & Ley, 2002; Martínez-Lostao *et al*, 2015; Farhood *et al*, 2019). Owing to the critical role of CTLs in cancer immunotherapy, a rapidly increasing number of immunotherapeutic studies have been launched focusing on reversing T-cell dysfunction to improve treatment outcome (Wherry & Kurachi, 2015; Zarour, 2016; Jiang *et al*, 2018; Thommen & Schumacher, 2018). However, tumor-intrinsic mechanisms, too, often contribute to the escape of immune surveillance, commonly impairing durable responses to ICB (Spranger *et al*, 2015; Gao *et al*, 2016; Zaretsky *et al*, 2016; Sharma *et al*, 2017; Litchfield *et al*, 2021; Vredevoogd *et al*, 2021; Zhang *et al*, 2022).

Among various resistance mechanisms, IFNγ signaling plays a crucial role in determining tumor sensitivity to T cells. For example, tumors with specific deficiencies in IFNγ signaling can be more resistant to immune checkpoint therapy (Gao *et al*, 2016; Zaretsky *et al*, 2016; Shin *et al*, 2017; Apriamashvili *et al*, 2022). Therefore, we previously set out to identify IFNγ signaling-independent tumor determinants of T-cell sensitivity. Specifically, we performed an unbiased genome-wide CRISPR-Cas9 knockout screen in IFNγ receptor-deficient (*IFNGR1*-KO) melanoma cells under cytotoxic T-cell attack, uncovering an important role of TRAF2 in determining tumor sensitivity to T-cell elimination in an IFNγ-independent tumor landscape (Vredevoogd *et al*, 2019). In the present study, we reanalyzed the results of this screen and identified TSC2 as a novel regulator of tumor cell sensitivity to T-cell killing, both *in vitro* and *in vivo*.

TSC1 and TSC2 are known to be crucial regulators of many biological processes by forming a complex that negatively regulates mTORC1 via the GTPase activation property of TSC2 toward RheB (Garami *et al*, 2003; Tee *et al*, 2003; Zhang *et al*, 2003; Inoki *et al*, 2003a). Their dysregulation contributes to tumor development (Adachi *et al*, 2003; Jiang *et al*, 2005; Menon & Manning, 2009; Xu

1 Division of Molecular Oncology and Immunology, Oncode Institute, The Netherlands Cancer Institute, Amsterdam, The Netherlands
2 Division of Tumor Biology and Immunology, The Netherlands Cancer Institute, Amsterdam, The Netherlands
*Corresponding author. Tel: +3120 512 2099; E-mail: d.peeper@nki.nl

et al, 2009). This correlates with elevated mTORC1 signaling (Inoki *et al*, 2002; Potter *et al*, 2002), which in turn leads to increased cell metabolism and biosynthesis while inhibiting autophagy, ultimately resulting in enhanced cell growth (Kim *et al*, 2002, 2011; Inoki *et al*, 2003b, 2006; Hosokawa *et al*, 2009; Düvel *et al*, 2010; Valvezan *et al*, 2017; He *et al*, 2018; Liu & Sabatini, 2020). However, how TSC1 and TSC2 regulate tumor vulnerability to T-cell toxicity has not yet been addressed to our knowledge. In addition to validating TSC2 as a key tumor cell determinant in the context of T-cell susceptibility, here we investigated its mechanism of action and its clinical relevance for cancer immunotherapy.

Results

Whole-genome CRISPR-Cas9 knockout screen identifies TSC2 as a negative regulator of tumor sensitivity to CTL killing

To identify critical factors protecting tumor cells against CTLs in addition to TRAF2 (Vredevoogd *et al*, 2019), we reanalyzed the data from our previous genome-wide CRISPR-Cas9 knockout screen (Fig 1A). The screen was performed in a human HLA-A*02:01$^+$/MART1$^+$ Interferon Gamma Receptor 1-knockout (*IFNGR1*-KO) D10 melanoma cell line that was challenged with healthy donor CD8 T cells, which were retrovirally transduced with a MART-1-reactive T-cell receptor (Gomez-Eerland *et al*, 2014). Tumor cells expressing sgRNAs targeting Tuberous Sclerosis Complex Subunit 1 or 2 (*TSC1* and *TSC2*) were significantly depleted from tumor cells under attack by MART-1-specific T cells, indicating that these genes contribute to tumor cell-intrinsic susceptibility to T cells (Fig 1B).

TSC1 and TSC2 act in a complex to inhibit mTORC1 activity. To validate these screen hits and assess their contributions to the sensitization to cytotoxic T cells, we first generated either single *TSC1*, *TSC2*, or *TSC1/TSC2* double knockout (KO) tumor cell lines. Because the screen was done in an *IFNGR1*-KO background, this was also the first setting we tested here. After differentially labeling non-targeting sgRNA-expressing cells (Ctrl) and TSC-KO cells with CFSE and CTV, respectively, they were mixed at a 1:1 ratio. This tumor cell mix was subsequently co-cultured with either nontumor-reactive (Ctrl) or MART-1-reactive CD8$^+$ T cells for three days. T-cell sensitivity was assessed by determining the ratio of Ctrl to TSC-KO tumor cells that survived at the end of co-culture (Fig 1C). Flow cytometry analysis showed that loss of *TSC2* alone or *TSC1/TSC2* double-KO significantly sensitized *IFNGR1*-KO melanoma cells to CTL killing to similar extents, whereas *TSC1*-KO alone showed a similar trend but was statistically insignificant (Figs 1D and E, and EV1A). This was likely caused by a slightly more stringent three-day continuous T-cell challenge used for the validation than the 24-h challenge in the screen. We interpret these results to suggest that TSC2 is the essential component of the TSC1-TSC2 complex that limits sensitivity to CTL attack in *IFNGR1*-deficient tumor cells. This aligns with the notion that TSC1 acts as a stabilizer of TSC2 instead of having a direct GTPase-activating function (Benvenuto *et al*, 2000; Chong-Kopera *et al*, 2006), limiting its dominance in the regulation.

To investigate whether these observations are dependent on the absence IFNγ signaling, we used IFNγ signaling-proficient cells. To avoid cell line bias, we used a cell line panel and performed the same competition assay, producing similar results (Fig 1F). Together, these results suggest a general and rate-limiting role of TSC2 in regulating tumor cells sensitivity to CTLs.

Tuberous Sclerosis Complex 2 accounts for the main functional activity in the TSC complex by acting as a GTPase-activating protein (GAP) for the small GTPase Rheb, a direct mTORC1 activator (Castro *et al*, 2003). Since the effect of *TSC2* inactivation was comparable with the combined knockout of both *TSC1* and *TSC2*, we decided to focus on the influence of *TSC2* depletion in the regulation of tumor cells to T-cell attack. The *TSC2*-depletion-induced CTL sensitization was validated with multiple *TSC2*-targeting sgRNAs (Fig EV1B and C). Further excluding sgRNA off-target effects, we reintroduced *TSC2* cDNA into *TSC2*-knockout melanoma cells (Fig 1G). This led to a rescue of the enhanced tumor sensitivity to CTL killing, demonstrating the dependence of this phenotype on TSC2 (Fig 1H). On the contrary, overexpression of TSC2 failed to cause CTL resistance. This suggests that TSC2 is required to protect tumor cells from CTL attack, but in isolation, is insufficient to cause resistance. We next validated the T-cell-sensitizing effect caused by *TSC2*-depletion in two human lung cancer cell lines (Fig 1I), as well as in B16 murine melanoma cells (Fig EV1D and E). The same effect can be seen from different cell viability assays where tumor cell lines were co-cultured with T cells separately, showing the absolute effect on individual tumor cell death (Fig EV1F). Of note, we observed a difference in cell viability between Ctrl and *TSC2*-KO tumors when a longer (five-day) assay was employed (Fig EV1G), indicating *TSC2* depletion influences tumor cell-intrinsic proliferation or survival. Therefore, to determine the net T-cell sensitization effect by *TSC2* depletion, all experiments were normalized to the tumor only condition. These results from different assays support our finding that *TSC2* ablation causes a general and robust sensitivity to T-cell cytotoxicity across different cell types of mouse and human origins.

TSC2 ablation sensitizes melanoma cells to CTL killing in an *in vivo* tumor ACT model

To assess the translational value of our *in vitro* findings, we next tested whether TSC2 deficiency can sensitize tumors to CTL-mediated tumor elimination *in vivo* as well. We performed an *in vivo* competition assay with a similar experimental setup to our *in vitro* competition assay, in which *TSC2*-KO and Ctrl melanoma cells expressing either mCherry or eGFP, respectively, were mixed at a 1:1 ratio. Next, they were subcutaneously transplanted into NOD severe combined immunodeficiency (SCID) gamma/B2m-deficient (NSG) mice (Fig 2A). Adoptive cell transfer (ACT) was performed with either Ctrl (non-matching) T cells or MART-1 T cells, after tumors had established. Mice treated with Ctrl T cells showed steady tumor outgrowth. By contrast, significant tumor control was observed in mice receiving MART-1 T-cell transfer, indicating the presence of an antigen-specific antitumor effect of ACT (Fig 2B). Tumor subpopulations that had survived the ACT were harvested and analyzed by flow cytometry. Of note, we also observed reduction in the *TSC2*-KO tumor population in the Ctrl T-cell-treated group, aligning with our observation during a longer five-day *in vitro* co-culture assay (Fig EV1G). Importantly, tumors treated with MART-1 T cells showed a significant depletion of *TSC2*-KO cells after normalization to the control T-cell-treated conditions

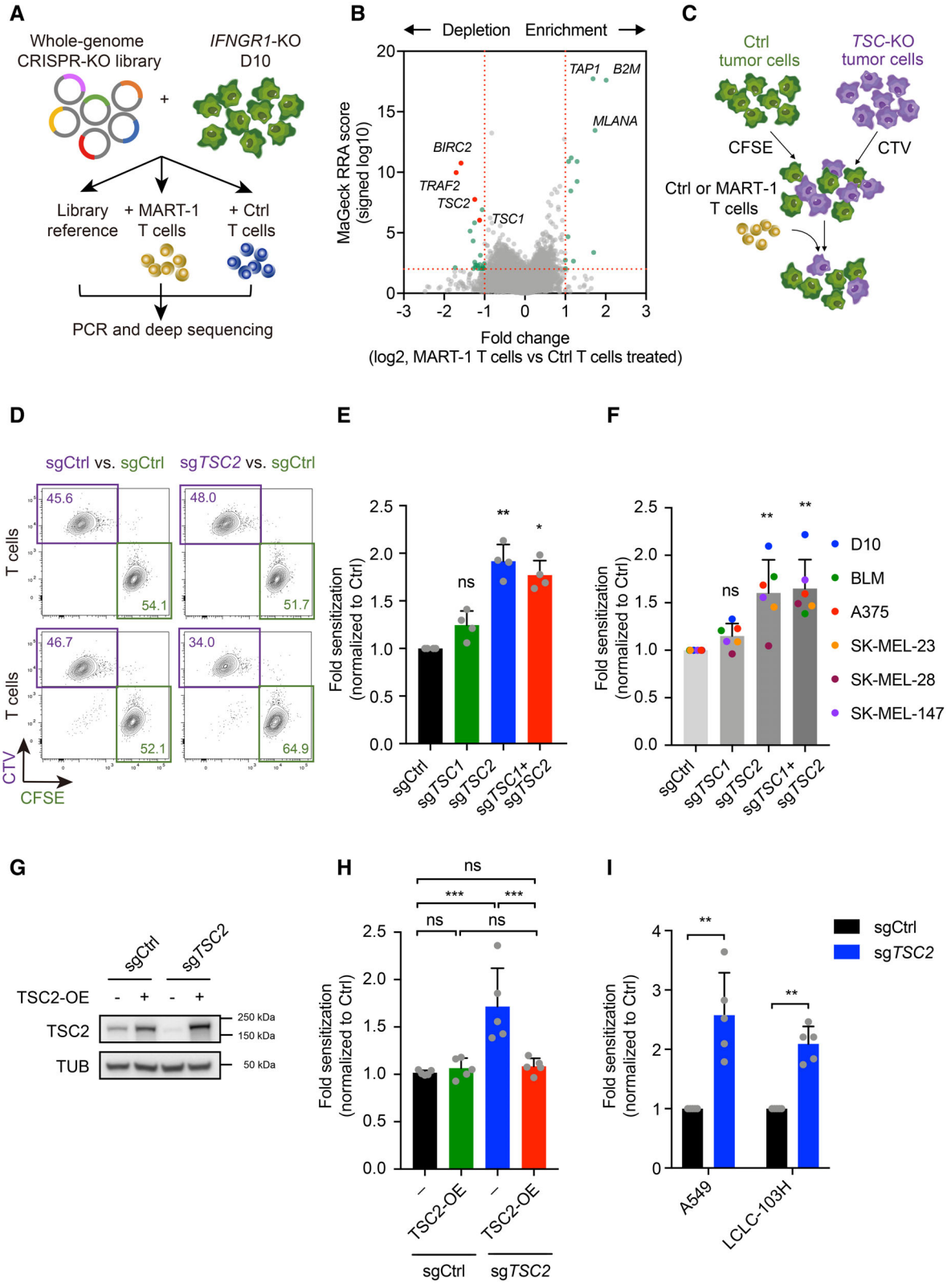
A
Whole-genome CRISPR-KO library
IFNGR1-KO D10
Library reference
+ MART-1 T cells
+ Ctrl T cells
PCR and deep sequencing
B
Depletion
Enrichment
MaGeck RRA score (signed log10)
TAP1
B2M
MLANA
BIRC2
TRAF2
TSC2
TSC1
Fold change (log2, MART-1 T cells vs Ctrl T cells treated)
C
Ctrl tumor cells
TSC-KO tumor cells
CFSE
CTV
Ctrl or MART-1 T cells
D
sgCtrl vs. sgCtrl
sgTSC2 vs. sgCtrl
Ctrl T cells
MART-1 T cells
45.6
54.1
48.0
51.7
46.7
52.1
34.0
64.9
CTV
CFSE
E
Fold sensitization (normalized to Ctrl)
ns
**
*
sgCtrl
sgTSC1
sgTSC2
sgTSC1+ sgTSC2
F
Fold sensitization (normalized to Ctrl)
ns
**
**
D10
BLM
A375
SK-MEL-23
SK-MEL-28
SK-MEL-147
sgCtrl
sgTSC1
sgTSC2
sgTSC1+ sgTSC2
G
sgCtrl
sgTSC2
TSC2-OE
- + - +
TSC2
TUB
250 kDa
150 kDa
50 kDa
H
ns
***
***
ns
ns
Fold sensitization (normalized to Ctrl)
–
TSC2-OE
–
TSC2-OE
sgCtrl
sgTSC2
I
**
**
Fold sensitization (normalized to Ctrl)
sgCtrl
sgTSC2
A549
LCLC-103H

Figure 1.

Figure 1. Whole-genome CRISPR-Cas9 knockout screen identifies TSC2 as a negative regulator of tumor sensitivity to CTL killing.

A Schematic outline of *in vitro* genome-wide CRISPR-Cas9 knockout screen in IFNγ receptor-deficient (*IFNGR1*-KO) D10 melanoma cells under CD8 T cell challenge (Vredevoogd *et al*, 2019).

B Volcano plot of depleted and enriched sgRNAs in tumor cells treated with MART-1 T cells versus Ctrl T cells.

C Schematic illustration of *in vitro* competition assay.

D Representative flow cytometry plot of *in vitro* competition assay (results are quantified in (E)).

E *In vitro* tumor T-cell co-culture competition assay in *IFNGR1*-KO D10 cells containing sgRNAs targeting *TSC1*, *TSC2* or both. Statistics was done by Kruskal–Wallis test with Dunn's *post hoc* test. Error bars indicate SD of four biological replicates with different T-cell donors ($n = 4$). *$P < 0.05$; **$P < 0.01$; ***$P < 0.001$; ****$P < 0.0001$.

F *In vitro* tumor T-cell co-culture competition assay in multiple melanoma cell lines containing indicated sgRNAs. Statistics was done by Kruskal–Wallis test with Dunn's *post hoc* test. Error bars indicate SD of six biological replicates with different cell lines ($n = 6$). *$P < 0.05$; **$P < 0.01$; ***$P < 0.001$; ****$P < 0.0001$.

G Western blot analysis of *TSC2* expression in cells used in (H).

H T-cell co-culture competition assay performed in sgCtrl- or sg*TSC2*-expressing D10 cells, and reconstituted with *TSC2* expression. Statistical analysis was performed with a one-way ANOVA, followed by a Tukey *post hoc* test. Error bars indicate SD of five biological replicates with different T-cell donors ($n = 5$). *$P < 0.05$; **$P < 0.01$; ***$P < 0.001$; ****$P < 0.0001$.

I *In vitro* T-cell co-culture competition assay of sgCtrl and sg*Tsc2*-expressing lung cancer cell lines. Statistics was done by Mann–Whitney test. Error bars indicate SD of five biological replicates with different T-cell donors ($n = 5$). *$P < 0.05$; **$P < 0.01$; ***$P < 0.001$; ****$P < 0.0001$.

Source data are available online for this figure.

(Fig 2C). In line with our *in vitro* results, the quantification of *in vivo* competition assay showed that tumor cells with *TSC2*-KO were considerably more vulnerable to $CD8^+$ T cells also *in vivo* (Fig 2D). The same effect was observed in an *in vivo* competition assay with reversed color labeling, excluding a label-specific effect (Fig EV2A–C). These results strengthen the notion that TSC2 serves a critical determinant of tumor sensitivity to CTL pressure.

TSC2 depletion-induced deregulation of mTOR signaling increases tumor cell death by CTL attack

While TSC1-TSC2 complex is known as a pivotal inhibitor of mTORC1 activity, it can also physically interact with mTORC2 (Frias *et al*, 2006; Huang *et al*, 2008), which in turn contributes to the phosphorylation of Akt, promoting cell proliferation and survival. Moreover, chronically activated mTORC1 signaling can attenuate PI3K/Akt downstream signaling, including cell survival and proliferation, serving as a negative feedback mechanism (Harrington *et al*, 2004; Shah *et al*, 2004). In agreement with the reported phenotype in melanocytes (Cao *et al*, 2017), we noted that *TSC2* ablation triggered an induction of mTORC1 signaling in multiple melanoma and lung cancer cell lines, as judged by the enhanced phosphorylation of ribosomal protein S6 at phospho-sites Ser235/236 and Ser240/244 (Fig 3A). This was accompanied by a more heterogeneous downregulation of mTORC2 signaling, as indicated by the suppression of phosphorylated Akt levels. A similar effect was observed in *TSC1* or *TSC1/TSC2* double knockout cells, but the effect was only minor in *TSC1*-KO alone (Fig EV3A), supporting the dominant role of TSC2 in regulating mTOR signaling. Importantly, regarding the heterogeneous mTORC2 regulation, we noted a consistently higher mTORC1:mTORC2 signaling ratio, as judged by the relative phosphorylation level of ribosomal protein S6 and Akt in *TSC2*-KO cells, indicating an mTORC1-skewing effect by *TSC2*-depletion (Figs 3B and EV3B). Of note, SK-MEL-28 cells, which are not sensitized upon *TSC2* ablation, did not show a sensitization effect during T-cell co-culture. Furthermore, they have the lowest mTORC1/mTORC2 ratio upon *TSC2* depletion, supporting our hypothesis that the mTORC1-skewing phenotype plays an important role in determining tumor sensitivity to CTL killing.

To better understand the dynamics mTORC1 and mTORC2 signaling in response to CTLs, particularly how they are affected by the absence of TSC2, we challenged either Ctrl or *TSC2*-KO tumor cells with MART-1 T cells and assessed the effects on mTOR signaling. In parental melanoma tumor cells challenged with MART-1 T cells, we observed a reduction in phosphorylated ribosomal protein S6 (phospho-Ser235/236, phospho-Ser240/244), which was accompanied by an upregulation of phospho-Ser473-Akt. However, TSC2-deficient tumor cells were less capable of regulating the phosphorylation level of these proteins upon CTL challenge (Fig 3C). This regulation was observed also in the A549 lung cancer cell line (Fig EV3C). This indicates that tumor cells respond to CTL challenge by redirecting their mTOR signaling toward a mTORC2-skewing phenotype, and that this regulation is impaired in *TSC2*-depleted tumor cells (Fig EV3D). These results suggest an important role of TSC2 in regulating tumor tolerance to T-cell attack via orchestrating the optimal ratio between mTORC1 and mTORC2 signaling.

Given these observations, we hypothesized that the shift toward mTORC1 signaling in *TSC2*-deficient tumor cells accounts for the sensitization toward CTL attack, whereas inhibiting mTORC1 reverses this phenotype. To test this, we treated T-cell-challenged *TSC2*-deficient melanoma cells with LY2584702, an inhibitor of the S6 kinase, a crucial node for mTORC1 signal relay (Meyuhas, 2008; Magnuson *et al*, 2012). This caused *TSC2*-deficient cells to show a marked decrease in phosphorylated ribosomal protein S6 (Fig EV3E). Taking into account that mTORC1 signaling is crucial for T-cell activation and development, we evaluated the impact of LY2584702 on T-cell cytotoxicity function after a three-day incubation in a matched tumor T-cell co-culture. We neither observed a significant T-cell viability impact, nor severe inhibition of T-cell cytotoxicity under these conditions (Fig EV3F). In line with the reduction in mTORC1 signaling, when LY2584702 was added during T-cell co-culture competition assay, the T-cell sensitization induced by *TSC2* depletion was partially rescued (Fig 3D). These results indicate that a TSC2-dependent orchestration of the mTORC1-mTORC2 signaling output contributes to modulating tumor cell sensitivity to CTLs.

Whereas mTORC1 activation stimulates cell growth by upregulating multiple biosynthesis processes and inhibiting autophagy, its inhibition protects cells from inflammation-induced apoptosis and senescence (Kakiuchi *et al*, 2019). Furthermore, mTORC2 activation induces cell survival through Akt-mediated inhibition of apoptosis (Kennedy *et al*, 1997). In agreement with this, we found that *TSC2*-

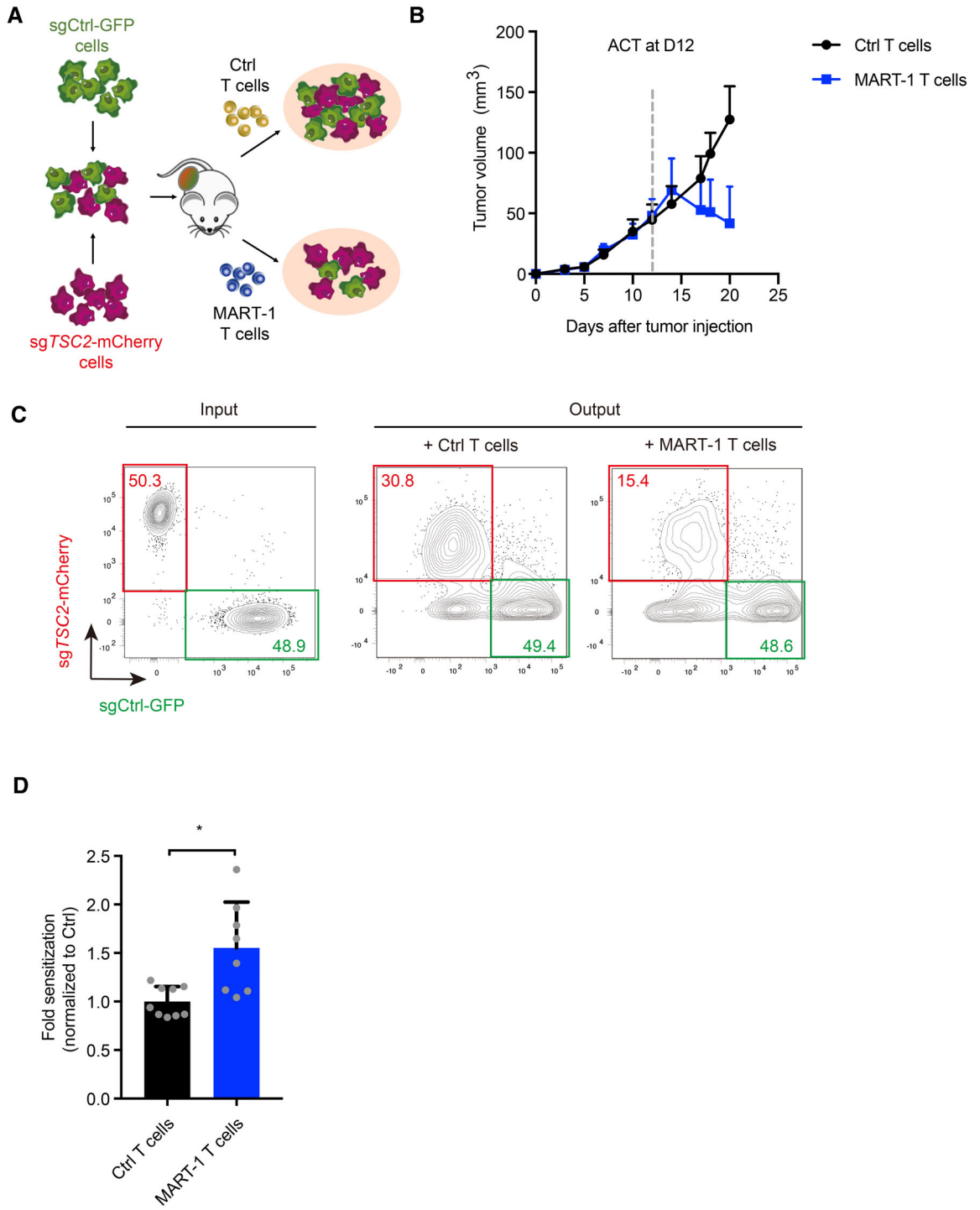

Figure 2. TSC2 ablation sensitizes melanoma cells to CTL killing in an *in vivo* tumor ACT model.

A Schematic outline of *in vivo* competition assay.

B Tumor growth upon adoptive cell transfer (ACT) with Ctrl ($n = 9$) or MART-1 ($n = 8$) T cells. Data points represent average tumor volume, and error bars represent SEM.

C Flow cytometry plot of both tumor mix input and representative output of the *in vivo* competition assay. Note that in bulk tumor digest nontumor tissue, such as stroma cells, express neither GFP nor mCherry, showing up in the flow cytometry plots as double-negative cells.

D Quantification of the *in vivo* competition assay (output) at end point by flow cytometry analysis. Error bars indicate SD. Statistical analysis was performed by Mann–Whitney test. *$P < 0.05$; **$P < 0.01$; ***$P < 0.001$; ****$P < 0.0001$. For this specific experiment, mice that deceased before the analysis ($n = 1$, Ctrl T-cell group), with failed ACT injection ($n = 1$, MART-1 T-cell group) or were completely tumor-free after ACT ($n = 1$, MART-1 T cell group) were excluded from the analysis.

Source data are available online for this figure.

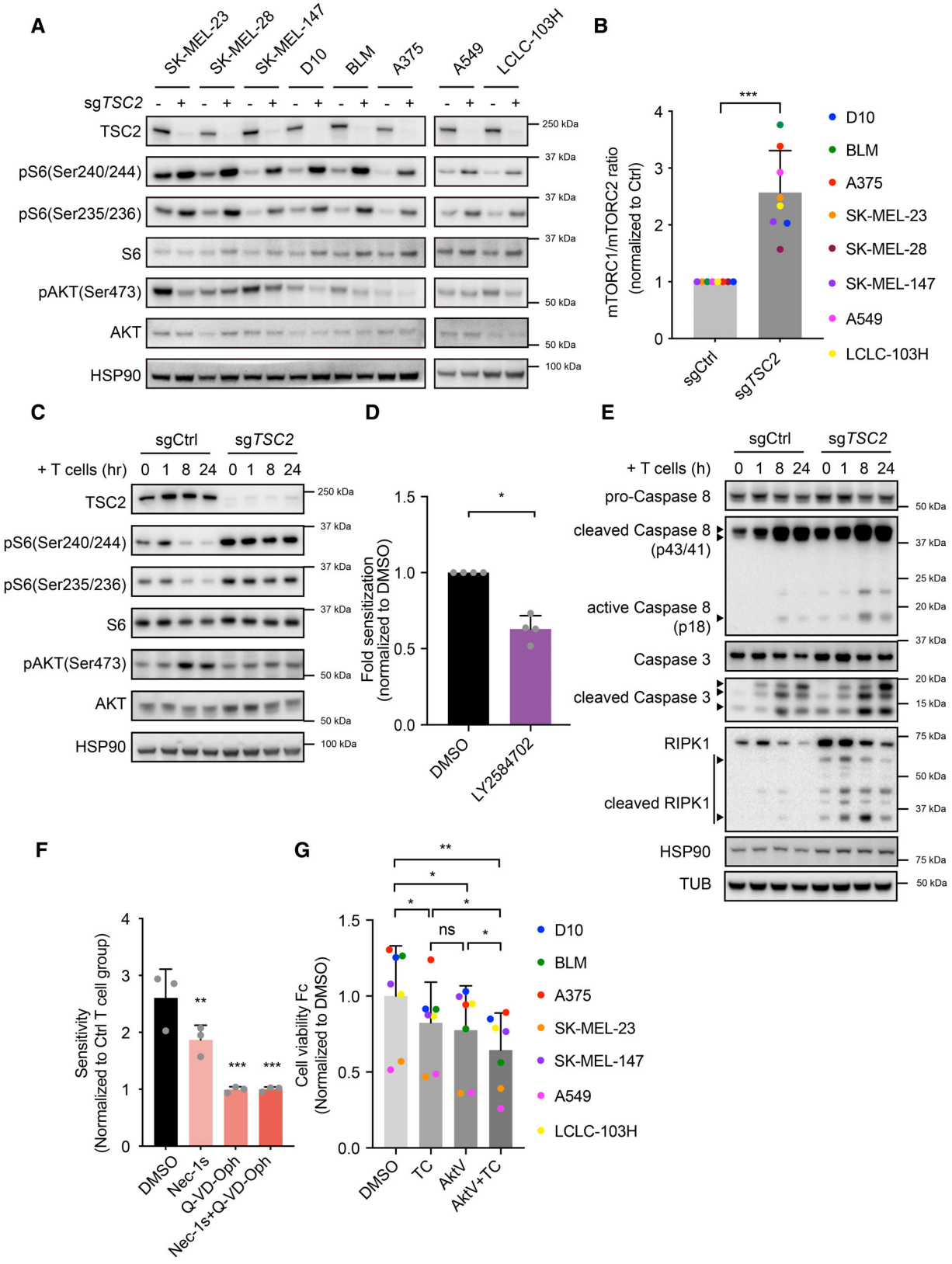

Figure 3.

Figure 3. *TSC2* depletion-induced deregulation of mTOR signaling increases tumor cell death by CTL attack.

A Western blot analysis of baseline mTOR signaling in sgCtrl- or sg*Tsc2*-expressing melanoma and lung cancer cell lines. Representative plot of 2–6 independent experiments. All blots shown in this panel were run in parallel.

B Pooled data of Western blot quantification on mTORC1/mTORC2 signaling ratio from all eight cell lines show in Fig EV3B. Statistical analysis was performed by Mann–Whitney test. Error bars indicate SD of mTOR ratio from eight different cell lines, with more than three independent experiments per cell line ($n = 8$). *$P < 0.05$; **$P < 0.01$; ***$P < 0.001$; ****$P < 0.0001$.

C Western blot analysis of mTOR signaling in sgCtrl- or sg*TSC2*-expressing D10 melanoma cells upon MART-1 T cell challenge for indicated time. Representative of three biological replicates with different T cell donors ($n = 3$).

D *In vitro* competition assay of sgCtrl- and sg*TSC2*-expressing D10 cells co-cultured with MART-1 T cells in the presence of LY2584702 (5 μM), normalized to DMSO-treated groups. Statistical analysis was performed by Mann–Whitney test. Error bars indicate SD of four biological replicates with different T cell donors ($n = 4$). *$P < 0.05$; **$P < 0.01$; ***$P < 0.001$; ****$P < 0.0001$.

E Western blot analysis of sgCtrl- or sg*TSC2*-expressing D10 melanoma cells upon MART-1 T cell challenge for indicated time. Representative of three biological replicates with different T cell donors ($n = 3$).

F *In vitro* competition assay of sgCtrl- and sg*Tsc2*-expressing D10 cells co-cultured with MART-1 T cells in the presence of necroptosis (Nec1-s, 20 μM) or apoptosis inhibitors (Q-VD-Oph, 50 μM), normalized to inhibitor plus Ctrl T cell-treated groups, showing the net MART-1 T-cell effect. Statistical analysis was performed by one-way ANOVA with Holm–Sidak's multiple comparisons test. Error bars indicate SD of three biological replicates with different T-cell donors ($n = 3$). *$P < 0.05$; **$P < 0.01$; ***$P < 0.001$; ****$P < 0.0001$.

G Cell viability analysis by CellTiter-Blue assay of T-cell sensitivity in multiple melanoma and lung cancer cell lines in the presence of Tautomycin (TC, 150 nM), Akt Inhibitor V (AktV, 1.5 μM), or the combination (TC, 150 nM$^+$ AktV, 1.5 μM) compared to DMSO-treated group. Statistical analysis was performed with a one-way ANOVA, followed by a Tukey's *post hoc* test. Error bars indicate SD of independent experiments with seven different cell lines. Each data point represents the average mean from three biological replicates with different T-cell donors ($n = 3$). *$P < 0.05$; **$P < 0.01$; ***$P < 0.001$; ****$P < 0.0001$.

Source data are available online for this figure.

KO cells showed enhanced baseline apoptosis with a stronger expression of cleaved RIPK, caspase 3 and caspase 8, which was further enhanced upon T-cell challenge (Fig 3E). The same result was observed when performing Incucyte analysis, in which an induction of caspase 3/7 staining was found in *TSC2*-KO tumor cells, which was enhanced upon T-cell treatment (Fig EV3G). In addition to apoptosis, mTORC1 inhibition also protects cells from necroptosis (Abe *et al*, 2019), which serves as an alternative cell death signaling. By performing the competition assay in the presence of either a necroptosis specific inhibitor (Nec-1s), an apoptosis inhibitor (Q-VD-Oph) or both, we found that *TSC2*-depletion-induced-T-cell sensitivity was abolished by blocking apoptosis signaling, which was partially rescued by necroptosis inhibition (Fig 3F). This indicates that *TSC2*-KO cells are more vulnerable to both apoptosis- and necroptosis-induced cell death. Together, these results suggest that TSC2 protects tumor cells from T-cell-induced cell cytotoxicity by orchestrating a pro-survival/anti-apoptotic mTOR response.

Because a TSC2 inhibitor is not available, we explored the potential translational value of modulating mTOR signaling for immunotherapy by other means. By treating tumor cells with a combination of a phosphatase inhibitor (tautomycin (TC)) and an Akt inhibitor (Triciribine (AktV)), we aimed to increase S6 phosphorylation (mTORC1 activation) and reduce Akt phosphorylation (mTORC2 inhibition). Indeed, the combination treatment led to simultaneous induction of S6 phosphorylation and potent suppression of Akt phosphorylation, producing a mTORC1-skewing phenotype similar to what was seen for *TSC2* depletion (Fig EV3H and I). Strikingly and in accordance with the *TSC2*-KO phenotype, pharmacological modulation of mTOR signaling was accompanied by an increased sensitivity to T-cell killing; this was seen in several tumor cell lines (Fig 3G). Taken together, these results indicate that tumor cells adapt to cytotoxic T-cell attack by shifting the balance of mTOR signaling toward increased mTORC2 activity to circumvent apoptosis and necroptosis. By reversing this balance, either through genetic inactivation of *TSC2* or through pharmacological modulation of mTOR signaling, tumor cell sensitivity to CTL attack can be augmented.

TSC2 depletion enhances TRAIL receptor expression and sensitizes melanoma cells to TRAIL-induced death

Antigens presented by tumor cells can stimulate specific CTL killing. To study whether *TSC2* depletion induces CTL sensitivity by modulating antigen presentation, we measured the expression of HLA-A*02:01 on Ctrl and *TSC2*-KO tumor cells, which present tumor Melan-A/MART-1 antigen recognized by MART-1-specific T cells. We observed a general HLA-A*02:01 induction on tumor cells co-cultured with MART-1 T cell, but not Ctrl T cells. A moderately higher HLA-A*02:01 expression was seen in *TSC2*-KO tumors only at baseline in the absence of antigen-specific T cells. However, no significant HLA-A*02:01 expression difference was found between Ctrl and *TSC2*-KO tumor cells after MART-1 T-cell co-culture (Fig EV4A). In addition, T-cell activation was unaltered, as judged by the comparable CD69 induction between MART-1 T-cells co-cultured with Ctrl and *TSC2*-KO tumors (Fig EV4B). These results suggest that increased antigen presentation and tumor antigenicity are unlikely important causes of *TSC2*-KO induced CTL sensitivity. In response to antigenic stimulation, CD8$^+$ T cells produce and secrete various effector cytokines that contribute to induction of cell death (Russell & Ley, 2002; Martínez-Lostao *et al*, 2015; Farhood *et al*, 2019). To dissect which of those are crucial in sensitizing *TSC2*-depleted tumor cells to CTLs, we treated either Ctrl or *TSC2*-KO tumor cells with different cytokines secreted by CTLs. We found that *TSC2*-KO cells were consistently more sensitive to TRAIL treatment (Figs 4A and EV4C and D). A similar sensitizing effect was achieved by treatment with a human TRAIL monoclonal agonist antibody (Conatumumab; Fig 4B). We cannot exclude sensitizing effects to additional cytokines upon *TSC2*-KO, and that the regulation may be cell line-dependent.

In *in vitro* T-cell tumor co-cultures, we observed upon tumor-antigen stimulation a strong induction of membrane-bound TRAIL on the cell surface of MART-1 T cells, but not Ctrl T cells, confirming the role of TRAIL in antigen-stimulated tumor killing (Fig EV4E). TRAIL potently induces cell apoptosis by binding to the two death receptors, TRAIL-R1 (encoded by *TNFRSF10A*) and

TRAIL-R2 (encoded by *TNFRSF10B*; Wang & El-Deiry, 2003). To assess whether *TSC2* inactivation affects the expression of these receptors, we determined their expression on multiple Ctrl and *TSC2*-KO tumor cell lines by flow cytometry. This revealed markedly elevated levels of either TRAIL-R1, TRAIL-R2, or both (Figs 4C and EV4F). To evaluate the importance of TRAIL

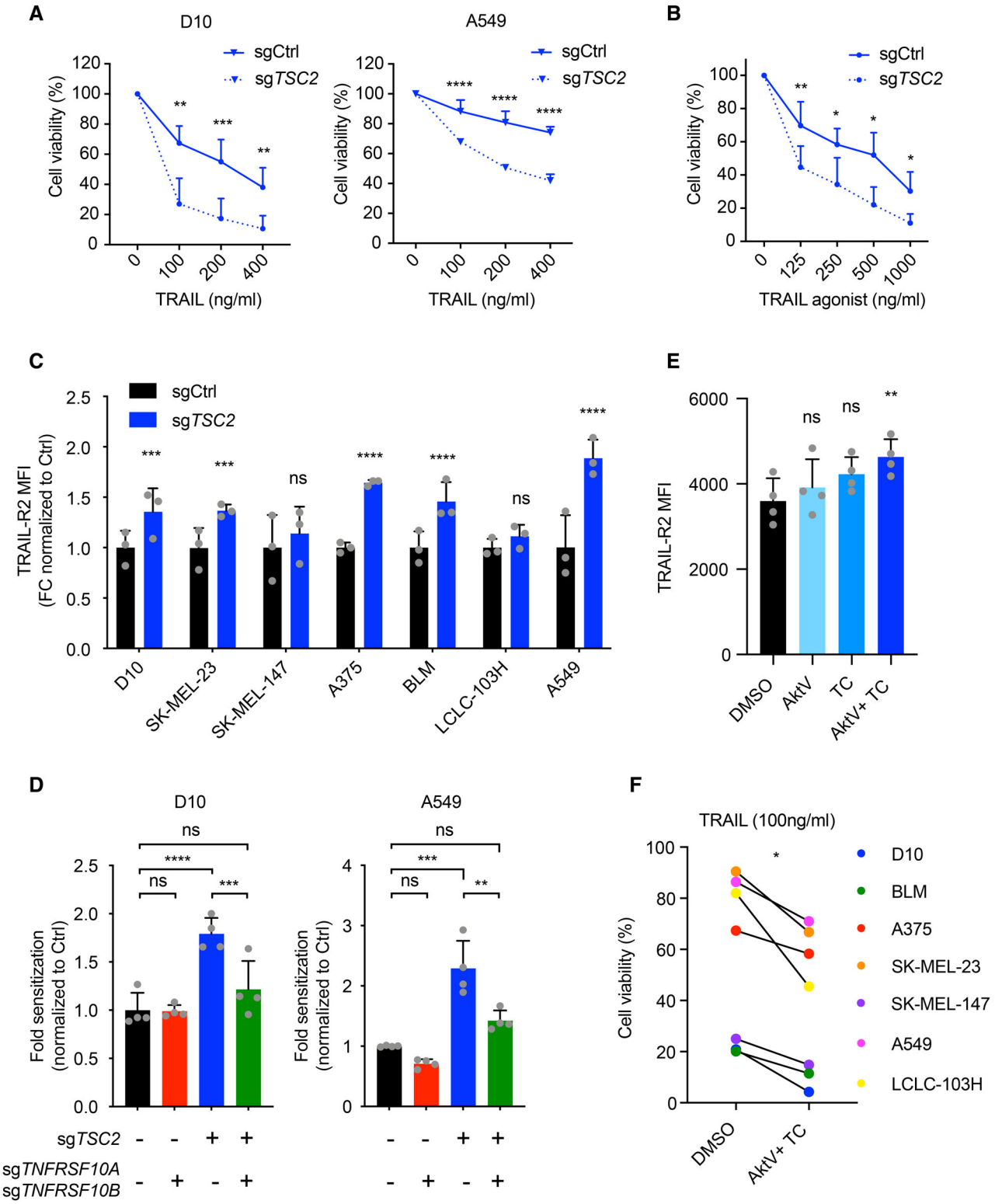

Figure 4.

Figure 4. *TSC2* depletion enhances TRAIL receptor expression and sensitizes melanoma cells to TRAIL-induced death.

A Cell viability analysis by CellTiter-Blue assay of sgCtrl- or sgTSC2-expressing D10 melanoma and A549 lung cancer cells treated with TRAIL at indicated concentrations for three days. Statistical analysis was performed by two-tailed unpaired Student's *t*-test. For D10, error bars represent SD from three independent experiments ($n = 3$). For A549, error bars represent SD of pooled data from two independent experiments with three technical replicates each ($n = 2$). *$P < 0.05$; **$P < 0.01$; ***$P < 0.001$; ****$P < 0.0001$.

B Cell viability analysis by CellTiter-Blue assay of sgCtrl- or sg*TSC2*-expressing D10 melanoma cells treated with TRAIL agonistic antibody Conatumumab, at indicated concentrations for two days. Statistical analysis was performed by two-tailed paired Student's *t*-test. Error bars indicate SD from three biological replicates ($n = 3$). *$P < 0.05$; **$P < 0.01$; ***$P < 0.001$; ****$P < 0.0001$.

C Flow cytometry analysis of TRAIL-R2 surface expression level in multiple sg*TSC2*- expressing tumor cell lines compared to their sgCtrl-expressing controls. Statistical analysis was performed by two-way ANOVA with Sidak's multiple comparisons test. Error bars represent SD of three biological replicates ($n = 3$). *$P < 0.05$; **$P < 0.01$; ***$P < 0.001$; ****$P < 0.0001$.

D *In vitro* competition assay performed by mixing control and tumor cells with ablation for either *TSC2*, TRAIL receptors (*TNFRSF10A* and *TNFRSF10B*), or both in a co-culture with MART-1 T cells. Statistical analysis was performed with a one-way ANOVA, followed by a Tukey's *post hoc* test. Error bars indicate SD of four biological replicates with different T-cell donors. *$P < 0.05$; **$P < 0.01$; ***$P < 0.001$; ****$P < 0.0001$.

E Flow cytometry analysis of TRAIL-R2 surface expression level in D10 melanoma cells after a three-day treatment with Tautomycin (TC, 150 nM), Akt Inhibitor V (AktV, 1.5 μM), or the combination (TC, 150 nM + AktV, 1.5 μM) compared to DMSO-treated cells. Statistical analysis was performed with a one-way ANOVA, followed by a Tukey's *post hoc* test. Error bars indicate SD of four biological replicates ($n = 4$). *$P < 0.05$; **$P < 0.01$; ***$P < 0.001$; ****$P < 0.0001$.

F Cell viability analysis by CellTiter-Blue assay of TRAIL (100 ng/ml) sensitivity in multiple parental melanoma and lung cancer cell lines in the presence of Tautomycin (TC, 150 nM) and Akt Inhibitor V (AktV, 1.5 μM) treatment, compared to DMSO-treated group. Statistical analysis was performed by Wilcoxon matched-pairs signed rank test of seven different cell lines. Representative graph of three biological replicates ($n = 3$). *$P < 0.05$; **$P < 0.01$; ***$P < 0.001$; ****$P < 0.0001$.

Source data are available online for this figure.

signaling in *TSC2*-depletion-induced-T-cell sensitivity, competition assays were performed in the context of disrupted TRAIL signaling by knocking out both *TNFRSF10A* and *TNFRSF10B*. This perturbation diminished the sensitizing effect caused by *TSC2* depletion (Fig 4D), establishing the requirement of TRAIL signaling in this setting. In line with the enhanced apoptosis in *TSC2*-KO tumor cells upon T-cell attack, we found that when blocking TRAIL signaling alone by depleting TRAIL-R during T-cell attack, the enhanced apoptosis in *TSC2*-KO tumor cells was rescued (Fig EV4G). Interestingly, when TRAIL signaling was blocked in the cell line SK-MEL-147, which shows no induction of TRAIL-R expression upon *TSC2*-KO (Figs 4C and EV4F), the induced T-cell sensitization could not be rescued (Fig EV4H). These results support our finding that enhanced TRAIL signaling plays an important role in *TSC2*-depletion-induced T-cell sensitivity. Moreover, when pharmacologically modulating mTOR signaling by TC/AktV combination treatment, we observed a significant induction of TRAIL-R2 surface expression (Fig 4E), whereas no significant increase was seen in both single inhibitor treatment groups. This illustrates the role of mTOR signaling balance in regulating TRAIL-R expression. Importantly, the TC/AktV combination treatment further sensitized multiple tumor cell lines to TRAIL-induced cell death (Fig 4F). Of note, as the same dosage was used for all cell lines, which show different TRAIL sensitivity windows, the result indicates an overall TRAIL-sensitizing effect upon AktV/TC treatment. It does not allow for comparing effect sizes between cell lines. These findings suggest crosstalk between mTOR and TRAIL signaling, where the mTORC1-skewing phenotype upon *TSC2*-depletion sensitizes tumor cells to TRAIL-induced cell death via upregulating TRAIL-R expression and inducing cell apoptosis.

Low *TSC2* expression: TRAIL Signaling ratio is associated with immune checkpoint blockade response in melanoma patients

Because *TSC2* depletion in tumor cells increases mTORC1 activity and elevates TRAIL receptor expression, which in turn sensitizes tumor cells to T-cell cytotoxicity, we next wished to explore any clinical implications. Examining the hallmark gene sets in The Cancer Genome Atlas (TCGA) analysis of melanoma, we found a negative correlation between *TSC2* expression and mTORC1 signaling, confirming the established function of TSC2 in mTOR regulation. Furthermore, *TSC2* expression levels negatively correlated with those of TRAIL receptors (*TNFRSF10A* and *TNFRSF10B*), as well as of TRAIL signaling (Fig 5A), in line with our findings above. Similar correlations were noticed among different cancer patient cohorts (Fig EV5A), indicating a more conserved role of TSC2 in TRAIL signaling regulation among different cancer types. To explore the influence of *TSC2* expression in cancer progression, we analyzed patient survival data from the TCGA melanoma cohort based on *TSC2* expression levels. Patients with melanomas expressing low levels of *TSC2* expression showed significantly prolonged disease-specific and progression-free survival (Fig EV5B). This association, while being subject to many factors including baseline immune pressure, is in agreement with our observation that TSC2 protects cells from apoptosis-/necroptosis-induced cell death.

Our findings indicate that upon *TSC2* ablation, tumor cells induce their expression of TRAIL receptors, thereby increasing their susceptibility to T-cell- or TRAIL-induced cell death. Therefore, we hypothesized that patients with lower *TSC2* expression (i.e., with higher TRAIL receptor expression) together with a stronger baseline TRAIL signaling may be more sensitive to cancer immunotherapy and show better treatment outcome. To test this, we analyzed cohorts of melanoma patients before receiving ICB therapy. Indeed, we found that patients with a lower *TSC2* expression: TRAIL signaling ratio responded significantly better to ICB therapy (Fig 5B; Riaz *et al*, 2017; Gide *et al*, 2019). Of note, in the Gide dataset, this ratio was significant only when patients were treated with both anti-PD-1 and anti-CTLA-4, likely triggering stronger immune pressure. These results indicate a correlation between the ratio of *TSC2* expression and TRAIL signaling and ICB treatment response of melanoma patients.

Lastly, in addition to *TSC2* single gene expression, we examined whether a TSC2 regulatory response upon immune challenge has any impact on ICB treatment outcome. We generated a TSC2

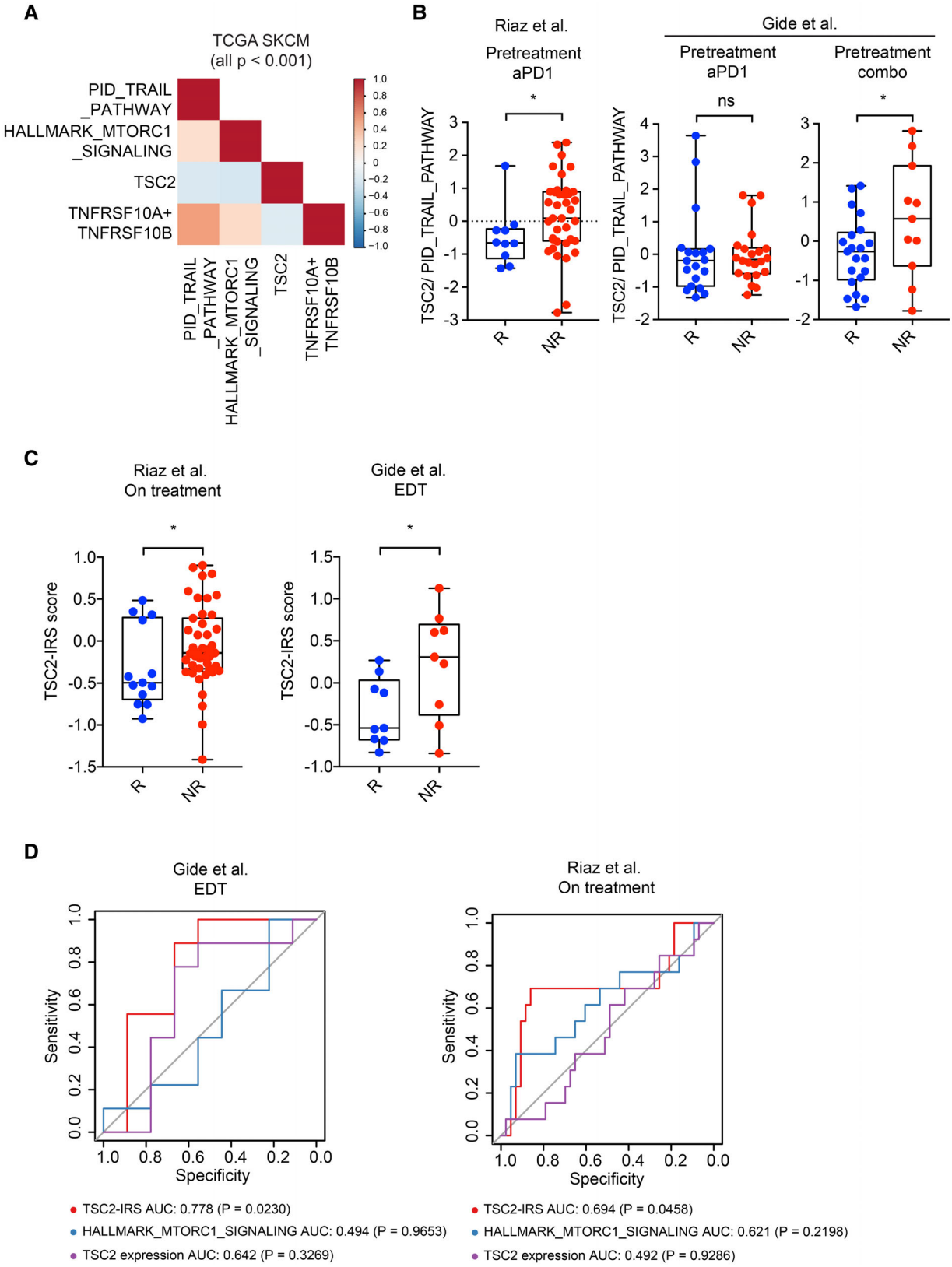

Figure 5.

Figure 5. Low *TSC2* expression: TRAIL signaling ratio is associated with immune checkpoint blockade response in melanoma patients.

A Heat-map of Spearman correlation between *TSC2*, *TNFRSF10A/ TNFRSF10B* expression, mTORC1, and TRAIL signaling in TCGA SKCM (Skin Cutaneous Melanoma) baseline patient cohort. HALLMARK_MTORC1_SIGNALING (Liberzon *et al*, 2015), PID_TRAIL_PATHWAY (Schaefer *et al*, 2009) gene sets were taken from the Molecular Signatures Database (MSigDB).

B *TSC2* expression: TRAIL signaling expression ratio for predicting ICB treatment responses in pre-treatment patient samples (Riaz *et al*, 2017; Gide *et al*, 2019). Combo, anti-PD-1 plus anti-CTLA-4 combination treatment. Statistical significance was calculated with Student's *t*-test for normally distributed data, or with Mann–Whitney test for non-normally distributed data. $*P < 0.05$; $**P < 0.01$; $***P < 0.001$; $****P < 0.0001$.

C TSC2 immune challenge signature expression in cohorts of patients after ICB treatment. Early during treatment (EDT), anti-PD-1 + anti-CTLA-4, and anti-PD-1 alone treatment cohorts. Statistical significance was calculated with Student's *t*-test for normally distributed data, or with Mann–Whitney test for non-normally distributed data. $*P < 0.05$; $**P < 0.01$; $***P < 0.001$; $****P < 0.0001$.

D ROC curve analysis showing the probability of the indicated signatures as classifiers of ICB treatment response. Statistical significance between signatures and no predictive value (AUC = 0.5) was calculated with bootstrapping. Partial response and complete response (PRCR) are defined as responder (R); stable disease (SD) and progressive disease (PD) are defined as nonresponder (NR).

Source data are available online for this figure.

Immune Response Signature (TSC2-IRS) from differentially expressed genes between control and *TSC2*-depleted tumor cell lines under either MART-1 T cell or TRAIL treatment. The TSC2-IRS was defined by the ratio of the differentially up- and down-regulated genes that overlapped between the two treatments (Fig EV5C). We analyzed the TSC2-IRS expression level in ICB-treated melanoma patient cohorts and found that responders showed a significantly lower TSC2-IRS expression (Fig 5C). Moreover, TSC2-IRS expression significantly distinguished responding from non-responding patients, whereas *TSC2* single gene expression or mTORC1 signaling from the hallmark gene sets alone failed to do this (Fig 5D). These clinical data point to a role for immune-induced TSC2 signaling in regulating tumor ICB response, supporting our functional data that *TSC2* inactivation augments tumor sensitivity toward immune pressure.

Discussion

By re-interrogating the hits from a genome-wide CRISPR-Cas9 knockout screen we performed previously for critical determinants of tumor cell sensitivity to T-cell killing (Vredevoogd *et al*, 2019), we identify here two negative mTOR regulators from the TSC complex, TSC1 and TSC2. Although these genes are established as tumor suppressors, their roles in determining tumor sensitivity to cytotoxic T-cell challenge have not yet been described to our knowledge. We show that TSC2 plays a dominant role over TSC1 in regulating tumor T-cell sensitivity and that this regulation is conducted, at least in part, through its control of mTORC1 and mTORC2 signaling balance; this regulation is impaired in *TSC2*-KO tumor cells upon T-cell attack. We also demonstrate that by pharmacologically redirecting the mTOR downstream signal toward mTORC1 while inhibiting mTORC2 signaling (simultaneously sustaining phosphorylated ribosomal protein S6 and inhibiting Akt phosphorylation), tumor vulnerability to T-cell killing can be induced (Fig 6A–D).

Cancer cells often show elevated mTORC1 signaling (Sato *et al*, 2010; Gerlinger *et al*, 2012; Grabiner *et al*, 2014; Saxton & Sabatini, 2017), resulting in enhanced cell growth associated with accelerated protein synthesis and metabolism (Düvel *et al*, 2010). However, several studies have shown that when encountering stress signals, cells downregulate mTORC1 signaling to lower their energy consumption rate and release the inhibition of autophagy, allowing for resource turnover (Ng *et al*, 2011; Aramburu *et al*, 2014). At the same time, they upregulate mTORC2 survival signal to inhibit cell apoptosis. Aligning with this, we found that tumor cells skew their mTOR signaling toward a mTORC2 phenotype when responding to stress induced by T-cell challenge. This mTOR signaling regulation may allow tumor cells to balance their energy requirement and enhance apoptosis resistance to survive under unfavorable conditions.

Acting as the central regulator of both mTOR1 and mTORC2 signaling, the TSC1-TSC2 complex is considered to be a central integrator of external stress. It is essential for triggering proper stress responses through balancing the mTOR signaling level (Aramburu *et al*, 2014; Demetriades *et al*, 2014; Menon *et al*, 2014). TSC1-TSC2 complex inhibits mTORC1 signaling by regulating Rheb activity and activating mTORC2 signaling through direct interaction (Huang *et al*, 2008). It also plays a crucial role in the crosstalk between mTORC1 and mTORC2 signaling through PI3K/Akt feedback regulation. Thereby, Akt directly phosphorylates TSC2 to suppress the inhibitory function of TSC2 on Rheb and mTORC1, limiting TSC2's inhibition of mTORC1 signaling (Manning *et al*, 2002; Potter *et al*, 2002; Cai *et al*, 2006; Huang & Manning, 2009). In agreement with our observations in multiple tumor cell lines, *TSC2* depletion interrupts the feedback regulation of mTORC2/Akt on mTORC1 signaling, leading to constitutively hyperactivated mTORC1 while suppressing mTORC2 signaling. This result confirms the status of TSC2 as a core regulator of the mTOR signaling balance.

TSC-deficient cells are more vulnerable to various cell death stimuli due to the impaired autophagy function caused by constitutive mTORC1 activation, while they are highly apoptotic due to diminished Akt signaling (Ng *et al*, 2011). In this study, we show that once *TSC2*-ablated tumor cells encounter cytotoxic T-cell stress, they are less capable of downregulating mTORC1 signaling and upregulating mTORC2 signaling. As a result, *TSC2*-depleted cells continue to display a higher mTORC1/mTORC2 signaling ratio than *TSC2*-proficient tumor cells. Hyperactivated mTORC1 signaling is known to induce apoptosis owing to a constantly high metabolism rate and suppressed resource turnover from autophagy inhibition (Düvel *et al*, 2010; Ng *et al*, 2011). When treating *TSC2*-KO cells with LY2584702 (an S6 kinase inhibitor), we observed downregulation of mTORC1 signaling, which was associated with reduced T-cell sensitivity. Together with the established inhibition by mTORC1 of autophagy, our data support the finding that autophagy inhibition sensitizes tumor cells to T-cell killing (Lawson *et al*, 2020). On the contrary, *TSC2*-depletion directly inhibits

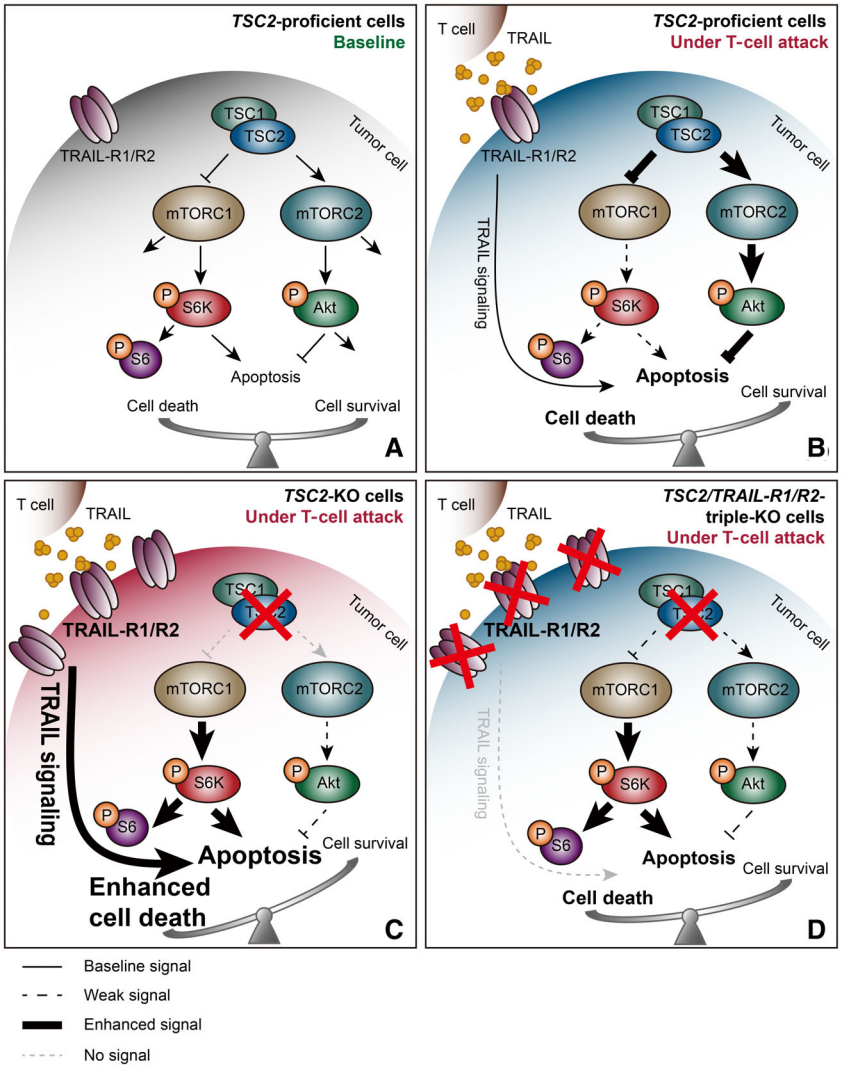

Figure 6. Modeling the role of TSC2 in governing tumor sensitivity to T-cell killing.

A At baseline, Tuberous Sclerosis Complex (TSC1/2) suppresses mTORC1 signaling while inducing mTORC2 signaling. These factors, and their respective downstream targets, affect several pathways. In this study, we focused on the balance of tumor cell apoptosis and survival in the context of cytotoxic T-cell attack.

B When challenged by cytotoxic T cells, tumor cells upregulate mTORC2 signaling and downregulate mTORC1 signaling, resulting in protection from cell death.

C Upon *TSC2* ablation, tumor cells (i) hyperactivate mTORC1 signaling, (ii) suppress mTORC2 signaling, and (iii) elevate TRAIL receptor expression. Together, these events lead to increased susceptibility to T-cell killing.

D When TRAIL-R1/R2 are ablated, *TSC2*-depleted tumor cells no longer receive extra TRAIL stimulation. As a consequence, only moderate cell killing is observed.

mTORC2, thereby releasing Akt-inhibited apoptosis (Kennedy *et al*, 1997), similar to what we observed in this study. Of note, we found Akt phosphorylation to be more heterogeneously regulated among different cancer cell lines. This may be caused by other regulators that phosphorylate Akt independently of TSC/mTORC2 signaling (Bozulic *et al*, 2008). Our study supports previous findings that TSC-null cells are extremely sensitive to multiple stress signals, such as DNA damage, ER stress, energy starvation, and apoptosis (Kang *et al*, 2010; Wang *et al*, 2013). Our results are also in line with the finding in TSC and Lymphangioleiomyomatosis (LAM) animal models that treatment with anti-PD-1 antibody or the combination of anti-PD-1 and anti-CTLA4 antibodies leads to the suppression of *TSC2*-null tumor growth and induces tumor rejection (Liu *et al*, 2018).

Mechanistically, we demonstrate that *TSC2*-depleted tumor cells are highly susceptible to TRAIL-induced cell toxicity through its binding to death receptors TRAIL-R1 and TRAIL-R2. Specifically, we found that *TSC2*-depleted tumor cells elevate their expression of TRAIL receptors. Correspondingly, by blocking TRAIL signaling during T-cell attack, increased T-cell sensitivity of tumor cells upon *TSC2*-depletion could be completely rescued. Our finding indicates the existence of crosstalk between TSC2/mTOR signaling and TRAIL sensitivity, which supports previous studies that activation of the Akt survival pathway leads to TRAIL resistance in tumor cells (Chen *et al*, 2001; Nesterov *et al*, 2001). Interestingly, loss of *TSC1/TSC2* was recently reported to induce tumor PD-L1 expression and increase tumor mutational burden, which was accompanied by an inflamed TME (Huang *et al*, 2022). Accordingly, *TSC1/TSC2*-

deficient tumors benefited from immunotherapy in murine models and NSCLC patient cohorts. Together with our finding, these studies indicate that TSC2 regulates tumor sensitivity to immune challenge, not only intrinsically by tuning tumor susceptibility to T-cell challenge, but also extrinsically by modulating PD-L1 expression and reshaping the TME. Both studies suggest that cancer patients with no or low TSC2 expression might benefit from immunotherapies.

Numerous mTOR inhibitors have been developed and are being tested for cancer treatment in the clinic (Chiarini *et al*, 2015; Hua *et al*, 2019). However, long-lasting anti-cancer effects are rare and patients often relapse due to various resistance mechanisms. Potential mechanisms have been suggested, including an activation of PI3K/Akt/mTORC2 survival signaling (Shi *et al*, 2005; Sun *et al*, 2005) and upregulation of PD-L1 expression in cancer cells (Lastwika *et al*, 2016; Deng *et al*, 2019). On the contrary, mTOR inhibition is associated with immunosuppressive properties, since both mTORC1 and mTORC2 are required for proper T-cell activation (Colombetti *et al*, 2006; Zheng *et al*, 2007) and trafficking (Sinclair *et al*, 2008). Moreover, mTORC1 and mTORC2 have distinct effects on fate decisions during immune cell differentiation (Delgoffe *et al*, 2009, 2011; Rao *et al*, 2010; Chi, 2012). These findings emphasize the importance of uncoupling mTORC1 and mTORC2 signaling in any future cancer treatment.

TRAIL agonists have shown promising clinical benefit in cancer treatment (Snajdauf *et al*, 2021). Combination therapies are being explored, for example with mTOR inhibitors, aiming to boost the effect of TRAIL (Snajdauf *et al*, 2021). In this study, we show that induction of tumor cell death by *TSC2* depletion could be recapitulated by treatment with Conatumumab, a TRAIL agonist monoclonal antibody that is being been evaluated in several clinical trials. This opens up a potential translational value of targeting TSC2 in combination with TRAIL cancer therapy. Although the detailed mechanism of how TSC2/mTOR signaling regulates TRAIL receptor expression remains to be explored, our finding provides in principle a rationale for selecting mTOR modulators as candidates for TRAIL combination therapy. Inhibiting mTOR signaling has a considerable impact on immune cell development and function (Dumont *et al*, 1990; Grolleau *et al*, 2002; Mills & Jameson, 2009). Therefore theoretically, targeting TSC2 in combination with TRAIL treatment may be sufficient to bypass the undesired immunosuppressive effect of combining mTOR inhibitors with ICB therapy, which is highly dependent on immune cell functions.

Overall, our study uncovers crosstalk between TSC2 regulation and TRAIL signaling and provides a novel concept for disrupting the mTORC1/mTORC2 balance to enhance tumor susceptibility to immune challenge. Further mechanistic study will be required to fully dissect the complexity of these signaling networks. This may allow us to identify specific targets for orchestrating an optimal mTORC1/2 signaling ratio in combination with TRAIL treatment in cancer therapy, aiming to avoid potential immunosuppressive effects.

Materials and Methods

Cell lines and cell culture

Human D10 (Zimmerer *et al*, 2013), SK-MEL-23 (CVCL_6027), SK-MEL-28 (CVCL_0526), SK-MEL-147 (CVCL_3876), A375 (CVCL_0132), BLM (CVCL_7035), LCLC-103H (CVCL_1375), and HEK293T (CVCL_0063) cell lines were retrieved from the Peeper laboratory cell line stock. A549 (CVCL_0023) cells were obtained from Prof. dr. Wilbert Zwart. Human melanoma and lung cancer cell lines without endogenous HLA-A*02:01 or MART-1 expression (SK-MEL-28, SK-MEL-147, A375, BLM, A549, LCLC-103H) were transduced with lentiviral constructs encoding both components. The B16-F10 (CVCL_0159) cell line was obtained from ATCC and was lentivirus-transduced to express the full-length ovalbumin (OVA) protein. OVA-expressing cells were selected with hygromycin (250 μg/ml, 10687010, Life Technologies). All cell lines were cultured in DMEM (GIBCO), supplied with 10% fetal bovine serum (Sigma) and 100 U/ml of Penicillin–Streptomycin (GIBCO). All cell lines were regularly tested for mycoplasma by PCR (Young *et al*, 2010) and were authenticated using the STR profiling kit from Promega (B9510).

Isolation, generation, and maintenance of MART-1 TCR CD8 T cells

MART-1 TCR CD8 T cells were generated as previously described (Vredevoogd *et al*, 2019). Briefly, primary human CD8 T cells were isolated from fresh, healthy male or female donor buffycoats (Sanquin, Amsterdam, the Netherlands), activated for 48 h in human CD8 T-cell media (RPMI Medium (GIBCO) containing 10% human serum (H3667, Sigma-Aldrich), 100 U/ml of Penicillin–Streptomycin, 100 U/ml IL-2 (Proleukin, Novartis), 10 ng/ml IL-7 (11340077, ImmunoTools), and 10 ng/ml IL-15 (11340157, ImmunoTools)) with plate-coated αCD3 and αCD28 antibodies (16-0037-85 and 16-0289-85, eBioscience) and spinfected with MART-1 TCR retrovirus on Retronectin coated (TB T100B, Takara) nontissue culture treated plates. Cells were harvested and maintained in human CD8 T-cell media 24 h after transduction. Paired untransduced T cells, which are isolated from the same donor but do not recognize MART-1 antigen, are used as control (Ctrl T cells). One week after retroviral transduction, MART-1 TCR expression was confirmed by flow cytometry (α-mouse TCR β chain, 553172, BD Pharmingen), and cells were cultured in RPMI containing 10% fetal bovine serum (Sigma), 100 U/ml of Penicillin–Streptomycin (GIBCO) and 100 U/ml IL-2 (Proleukin, Novartis).

Knockout and overexpression cell line generation

Knocking out and overexpressing genes of interest in different cell lines were done by lentiviral transduction. For gene knockouts, sgRNAs were cloned into lentiCRISPR-v2 (#52961, Addgene) plasmid using a SAM target sgRNA cloning protocol (S. Konermann, Zhang lab, 2014). For *TSC2* reconstitution, full-length *TSC2* cDNA containing a CRISPR-Cas9-resistant silent mutation was cloned into pCDH-blast plasmid. Lentivirus was produced by transfecting HEK293T cells with psPAX2 (#12260, Addgene) and pMD2.G (#12259, Addgene) using polyethylenimine. The media was refreshed with OptiMEM (31985062, GIBCO) containing 2% fetal bovine serum 24 h after transfection. Supernatant was harvested 72-h post-transfection, filtered and stored at −80°C. Tumor cells were transduced with lentivirus, together with polybrene (8 μg/ml), and cell media was refreshed 24 h later. Cells were selected with antibiotics for at least one week. *TSC1/TSC2* double knockout cells

or *TSC2* reconstitution in knockout cells were done sequentially by using both puromycin-selectable and blasticidin-selectable plasmids. *TNFRSF10A /TNFRSF10B* double knockout cells were purified by cell sorting after antibiotic selection.

sgRNA targeting sequences:
sg_hCtrl: 5′- GGTTGCTGTGACGAACGGGG -3′
sg_h*TSC1*: 5′- CGAGATAGACTTCCGCCACG -3′
sg_h*TSC2*-1: 5′- CAGAGGGTAACGATGAACAG -3′
sg_h*TSC2*-2: 5′- TCCTTGCGATGTACTCGTCG -3′
sg_h*TSC2*-3: 5′- ATTGTGTCTCGCAGCTGATG -3′
sg_h*TNFRSF10A*: 5′- AGCCTGTAACCGGTGCACAG -3′
sg_h*TNFRSF10B*: 5′- AGGTGGACACAATCCCTCTG -3′
sg_mCtrl: 5′- AAAAAGTCCGCGATTACGTC -3′
sg_m*Tsc2*-1: 5′- TCATTCGGATGCGATTGTTG -3′
sg_m*Tsc2*-2: 5′- AGTTCTTGAGAGAGTAGAGC -3′
sg_m*Tsc2*-3: 5′- GGTCAGCAGGTCATGGACGA -3′.

In vitro competition assay

Parental or gene-modified cells were stained with either the CellTrace CFSE Cell Proliferation Kit (C34554, CFSE; Thermo Scientific) or the CellTrace Violet Cell Proliferation Kit (C34557, CTV; Thermo Scientific) following the manufacturer's instructions. Stained cells were mixed at a 1:1 ratio and challenged with either MART-1 T cells or Ctrl T cells for 3 days. For drug treatment, indicated compounds were added in the media together with T-cell co-culture, LY2584702 (S7704, SelleckChem), Nec-1 s (50-429-70001, Sigma-Aldrich), and Q-VD-Oph (S7311, SelleckChem). For TRAIL treatment competition assay, 100 ng/ml sTRAIL/Apo2L (310-04, Peprotech) was added to the culture media. The percentage CFSE- and CTV-positive cells was analyzed by flow cytometry. Sensitivity was calculated by the ratio of control cells to gene-modified cells under MART-1 T-cell challenge normalized to their corresponding Ctrl T-cell condition to exclude tumor cell-intrinsic impact. Fold sensitization was calculated by further normalizing to the sgCtrl-sgCtrl tumor mixing or no treatment groups, as specified for each experiment.

In vitro cytotoxicity assay

1×10^4 tumor cells were seeded per well into 96-well culture plates (Greiner). Recombinant Human IFNα-1b (11343594, ImmunoTools), IFNβ-1b (11343543, ImmunoTools), IFNγ (Peprotech), TNFα (300-01A, Peprotech), TNFβ (300-01B, Peprotech), sFas Ligand (310-03H, Peprotech), sTRAIL/Apo2L (310-04, Peprotech), Tautomycin (580551, Sigma-Aldrich), Triciribine (Akt Inhibitor V, 124012, Merckmillipore), Conatumumab (TAB-203, Creative Biolabs Inc.) or T cells were added at indicated concentrations or ratio. Cells were incubated for 3 days before viability analysis unless specifically indicated. Drugs were washed away and cell viability was read using Cell Titer Blue Viability Assay (G8081, Promega) according to the manufacturer's instruction. For staining, plates were fixed and stained for 1 h with crystal violet solution (0.1% crystal violet (Sigma) and 50% methanol (Honeywell)). Quantification was done by dissolving remaining crystal violet in 10% acetic acid (Sigma). Absorbance of the solution was measured on an Infinite 200 Pro spectrophotometer (Tecan) at 595 nm. For Incucyte (Incucyte Zoom, Essen Bioscience) experiments, 1×10^4 tumor cells were seeded per well in 96-well culture plates (Greiner). CD8 T cells were added in indicated ratios and a Caspase-3/7 dye (4440, Sartorius) was added at 1:1,000 dilution. Growth of these co-cultures was followed for 72 h.

In vivo competition assay and mouse model

D10 cells were first lentivirally transduced with sgCtrl or sg*TSC2* and selected with puromycin for one week as described above. Then, cells were lentivirally transduced with eGFP (pLX304-EGFP-Blast) or mCherry (pLX304-mCherry-Blast) expression plasmids and sorted. Cells were mixed at 1:1 ratio prior to injection. 1×10^6 mixed cells per mouse were subcutaneously injected into immune-deficient NSG-B2m mice (n = 10, The Jackson Laboratory, Strain #:010636) with Matrigel (354230, Corning). Tumor growth was monitored three times per week. Mice were randomized 12 days after tumor injection based on tumor size and gender, and either 5×10^6 MART-1 or Ctrl (untransduced, non-matching) human CD8 T cells were intravenously injected into the tail vein, followed by daily 100,000 U IL-2 (Proleukin, Novartis) intraperitoneal injection for three consecutive days. Researchers were blinded for treatment given. Tumors were harvested 8-day post-ACT and digested into single cell suspensions. EGFP- and mCherry-positive cells were analyzed by flow cytometry. Mice without tumor outgrowth or failed to receive proper ACT were excluded.

Flow cytometry

For cell surface staining, cells were harvested and stained with fluorescent-conjugated antibodies. For cytokine production, cells were stimulated with 20 ng/ml PMA (P1585, Sigma) and 1 μg/ml Ionomycin (I9657, Sigma) for 4 h before harvesting for analysis, and Golgiplug (555029, BD Biosciences) was added 1 h after PMA/Ionomycin was added. Surface staining was performed by staining cells in PBS containing 0.1% Bovine Serum Albumin (Sigma) and fluorescent-conjugated antibodies for 30 min on ice. Intracellular staining was performed with Foxp3/transcription factor staining buffer set (00-5523-00, Life Technologies) according to the manufacturer's instructions. Annexin V staining was performed using Annexin Binding Buffer (V13246, ThermoFisher) according to the manufacturer's instructions. Samples were analyzed with Fortessa flow cytometer (BD Bioscience). Antibodies against human CD261 (307207, Biolegend), CD262 (307405, Biolegend), TRAIL (308205, Biolegend), CD69 (310914, Biolegend), HLA-A2 (561339, BD Biosciences), IFNγ (554702, BD Biosciences), TNFα (557068, BD Biosciences), Granzyme B (560213, BD Biosciences), IL-2 (500325, Biolegend) and Live/Dead Fixable Near-IR Dead Cell Stain Kit (L34976, Thermo) were used.

Immunoblotting

Cells were washed with PBS, scrape-harvested, and lysed for 30 min on ice with RIPA buffer (50 mM TRIS pH 8.0, 150 mM NaCl, 1% Nonidet P40, 0.5% sodium deoxycholate, 0.1% SDS) supplemented with Halt Protease and Phosphatase inhibitor cocktail (78444, Fisher Scientific) for phosphoprotein blotting. Samples were centrifugated at 17,000 *g*, supernatant was collected and protein concentration was measured by Bradford Protein Assay (500-0006, Bio-Rad). To prepare immunoblot samples, protein concentration was normalized

and 4×LDS sample buffer (15484379, Fisher Scientific) containing 10% β-Mercaptoethanol (final concentration 2.5%) was added, following by 5-min incubation at 95°C. Samples were size-separated on 4–12% NuPAGE Bis-Tris polyacrylamide-SDS gels (Invitrogen) and transferred on nitrocellulose membranes (IB301031, Invitrogen, iBlot™ Transfer Stack). Blots were blocked in 4% milk powder in 0.2% Tween/PBS (PBST) and incubated at 4°C overnight with primary antibodies. After washing by PBST, secondary antibodies were applied for 1 h at room temperature. Blots were then washed by PBST and developed with SuperSignal West Dura Extended Duration Substrate (34075, Thermo Scientific), and luminescence was captured Luminescence signal was detected by either Amersham Hyperfilm high-performance autoradiography film or Bio-Rad ChemiDoc imaging system with default settings. Primary antibodies against TSC1 (6935, Cell Signaling Technology), TSC2 (4308, Cell Signaling Technology), Akt (sc-8312, Santa Cruz Biotechnology), pAktSer473 (4060, Cell Signaling Technology), S6R (2217, Cell Signaling Technology), pS6Ser240/244 (2215, Cell Signaling Technology), pS6Ser235/236 (2211, Cell Signaling Technology), Caspase 3 (9665, Cell Signaling Technology), cleaved Caspase 3 (9664, Cell Signaling Technology), Caspase 8 (4790, Cell Signaling Technology), cleaved Caspase 8 (9748, Cell Signaling Technology), RIPK1 (3493, Cell Signaling Technology), Vinculin (4650, Cell Signaling Technology), α-Tubulin (T9026, Sigma), HSP90 (sc-7947, Santa Cruz Biotechnology), cyclophilin B (43603, Cell Signaling Technology) were used. Horseradish peroxidase-conjugated secondary antibodies against mouse IgG (G21040, Thermo Scientific), rabbit IgG (G21234, Invitrogen) were used.

Sample preparation for generating TSC2 immune challenge signature

D10 melanoma and A549 lung cancer cell lines expressing sgCtrl or sg*TSC2* were seeded into 10 cm tissue culture dishes at 70% for 48 h. Tumor cells were challenged with CFSE (423801, Biolegend) prelabeled MART-1 T cells, with T cell to tumor ratio causing 50% tumor cell killing, or sTRAIL/Apo2L (310-04, Peprotech; D10: 10 ng/ml; A549: 100 ng/ml) overnight. Supernatant containing cell debris and T cells was discarded and attached cells were harvested by trypsinization. Samples were washed with PBS and stained with DAPI. Pure viable tumor cells were sorted by FACSAria Fusion Cell Sorters gating on DAPI-, CFSE- populations and sent for RNA sequencing.

Whole-genome CRISPR-KO screen data analysis

Count data from the whole-genome screen (Vredevoogd *et al*, 2019) was reanalyzed using MAGeCK (v0.5.7) using the second best sgRNA method (Li *et al*, 2014). To make this analysis more robust, sgRNAs with low read counts (< 50) were filtered from this analysis.

Data resources and bioinformatic analysis

Count data of the TCGA SKCM patient cohort were obtained using the GDC query from the TCGAbiolinks package (1.15.1) in R (4.0.2). Read count data were preprocessed and normalized using DESeq2 (1.30.0). Expression data of the pan-cancer TCGA cohorts were obtained using query option on the cBioPortal website. Survival analysis was performed on the disease-specific survival (DSS) data and the progression-free interval (PFI) data in months (Liu *et al*, 2018), using the top and bottom quantiles of the *TSC2* expression for grouping the samples.

For the anti-PD-1-treated patient cohort (Riaz *et al*, 2017), the raw counts were downloaded from NCBI's GEO (GSE91061). For a second patient cohort, containing patients treated with either anti-PD-1 monotherapy or combined anti-PD-1 and anti-CTLA-4 (Gide *et al*, 2019), the RNA sequencing data were downloaded from the European Nucleotide Archive (ENA) under project PRJEB23709. The fastq files were mapped using STAR (2.6.0c) with default settings on two-pass mode. The raw counts were generated using HTSeq (0.10.0). For both cohorts, the raw read count data were preprocessed and normalized using DESeq2 (1.30.0). *Z*-scores were obtained from the normalized read counts by subtracting the row means and scaling by dividing the columns by the SD.

For the data on the control and *TSC2*-depleted cell lines after cytotoxic T cell or TRAIL challenge used for generating the TSC2 immune response signature (TSC2-IRS), the fastq files were mapped to the GRCh38 human reference genome (Homo.sapiens.GRCh38.v82) using STAR (2.7.3a) with default settings on two-pass mode. Count data were generated with HTSeq (0.12.4) and preprocessed and normalized using DESeq2 (1.30.0). The genes from the TSC2-IRS signature were significantly differentially expressed genes (DEGs) between the *TSC2*-depleted tumor cell lines versus the control tumor cell lines, and showed up in both T-cell treatment and TRAIL treatment groups. Significant DEGs were defined by an adjusted *P*-value of < 0.01 and a minimum fold change (fc) of 0.15 or maximum fc of −0.15, for genes that were either up or down in *TSC2*-depleted cell lines respectively. For clinical data analysis, TSC2-IRS expression score was generated by first calculating separately the average expression level of the up signature (consists of 44 upregulated genes) and down signature (consists of 78 downregulated genes), and then dividing the up by the down expression score.

Statistics

Sample size was estimated, and the number of samples used for each experiment is indicated. When comparing two groups, a Two-tailed Student's *t*-test was performed for normally distributed data, or by two-tailed Mann–Whitney test with Bonferroni correction for data that was not normally distributed. When comparing more than one group of data to one control group, one-way ANOVA with Holm–Sidak's multiple comparisons test was performed when data are normally distributed, or Kruskal–Wallis test with Dunn's *post hoc* test was used when data were not normally distributed. Tukey's *post hoc* analysis was used for multiple comparisons between all groups. Data distribution normality was analyzed by Shapiro–Wilk test. All analyses were performed by Prism (Graphpad Software Inc.). *P*-value lower than 0.05 was defined as statistically significant. For *in vivo* experiments, sample size estimation for experimental study design was calculated by G*Power (Faul *et al*, 2007).

Animal welfare

All animal studies were approved by the animal ethics committee of the Netherlands Cancer Institute (NKI) and performed under

approved NKI CCD (Centrale Commissie Dierproeven) projects according to the ethical and procedural guidelines established by the NKI and Dutch legislation. Male or female NSG-B2m (The Jackson Laboratory) mice were used after at 8 weeks or older. Mice were housed in one-time use standard cages at controlled air humidity (55%), temperature (21°C), and light cycle. All housing material, food, and water were autoclaved or irradiated before use.

Data availability

The MDAR guidelines have been followed for transparent reporting in manuscripts and other outputs. The RNA-Seq dataset used in this study to generate TSC2-IRS is available in the Gene Expression Omnibus (GEO) database (GSE201514), and assigned the links as below: https://www.ncbi.nlm.nih.gov/geo/query/acc.cgi?acc=GSE201514.

Expanded View for this article is available online.

Acknowledgements
We would like to thank all members in the Peeper laboratory, especially G. Apriamashvili, B. de Bruijn, O. Krijgsman, and T. Kuilman, and our colleagues in the Division of Molecular Oncology and Immunology for their valuable input. We would like to thank T. Schumacher and W. Zwart for sharing cell lines and input, R. Bernards for sharing Conatumumab and E. Henske for advice. Moreover, we would like to thank The Netherlands Cancer Institute Flow Cytometry facility, Genomic Core facility, Animal Laboratory for their contributions. This work was supported by Oncode Institute and The Dutch Cancer Society (KWF).

Author contributions
Chun-Pu Lin: Conceptualization; data curation; software; formal analysis; validation; investigation; visualization; methodology; writing – original draft; project administration; writing – review and editing. **Joleen J H Traets:** Software; formal analysis; writing – review and editing. **David W Vredevoogd:** Conceptualization; formal analysis; methodology. **Nils L Visser:** Resources. **Daniel S Peeper:** Conceptualization; resources; supervision; funding acquisition; investigation; methodology; project administration; writing – review and editing.

Disclosure and competing interests statement
DSP is a co-founder, shareholder, advisor of Immagene, and EMBO member, which is unrelated to this study. The other authors declare that they have no conflict of interest.

References

Abe K, Yano T, Tanno M, Miki T, Kuno A, Sato T, Kouzu H, Nakata K, Ohwada W, Kimura Y *et al* (2019) mTORC1 inhibition attenuates necroptosis through RIP1 inhibition-mediated TFEB activation. *Biochim Biophys Acta Mol Basis Dis* 1865: 165552

Adachi H, Igawa M, Shiina H, Urakami S, Shigeno K, Hino O (2003) Human bladder tumors with 2-hit mutations of tumor suppressor gene TSC1 and decreased expression of p27. *J Urol* 170: 601 – 604

Apriamashvili G, Vredevoogd DW, Krijgsman O, Bleijerveld OB, Ligtenberg MA, de Bruijn B, Boshuizen J, Traets JJH, D'Empaire Altimari D, van Vliet A *et al* (2022) Ubiquitin ligase STUB1 destabilizes IFNγ-receptor complex to suppress tumor IFNγ signaling. *Nat Commun* 13. https://doi.org/10.1038/s41467-022-29442-x

Aramburu J, Ortells MC, Tejedor S, Buxadé M, López-Rodríguez C (2014) Transcriptional regulation of the stress response by mTOR. *Sci Signal* 7: 1 – 12

Benvenuto G, Li S, Brown SJ, Braverman R, Vass WC, Cheadle JP, Halley DJJ, Sampson JR, Wienecke R, DeClue JE (2000) The tuberous sclerosis-1 (TSC1) gene product hamartin suppresses cell growth and augments the expression of the TSC2 product tuberin by inhibiting its ubiquitination. *Oncogene* 19: 6306 – 6316

Bozulic L, Surucu B, Hynx D, Hemmings BA (2008) PKBalpha/Akt1 acts downstream of DNA-PK in the DNA double-strand break response and promotes survival. *Mol Cell* 30: 203 – 213

Cai SL, Tee AR, Short JD, Bergeron JM, Kim J, Shen J, Guo R, Johnson CL, Kiguchi K, Walker CL (2006) Activity of TSC2 is inhibited by AKT-mediated phosphorylation and membrane partitioning. *J Cell Biol* 173: 279 – 289

Cao J, Tyburczy ME, Moss J, Darling TN, Widlund HR, Kwiatkowski DJ (2017) Tuberous sclerosis complex inactivation disrupts melanogenesis via mTORC1 activation. *J Clin Invest* 127: 349 – 364

Castro AF, Rebhun JF, Clark GJ, Quilliam LA (2003) Rheb binds tuberous sclerosis complex 2 (TSC2) and promotes S6 kinase activation in a rapamycin- and farnesylation-dependent manner. *J Biol Chem* 278: 32493 – 32496

Chen X, Thakkar H, Tyan F, Gim S, Robinson H, Lee C, Pandey SK, Nwokorie C, Onwudiwe N, Srivastava RK (2001) Constitutively active Akt is an important regulator of TRAIL sensitivity in prostate cancer. *Oncogene* 20: 6073 – 6083

Chi H (2012) Regulation and function of mTOR signalling in T cell fate decisions. *Nat Rev Immunol* 125: 325 – 338

Chiarini F, Evangelisti C, McCubrey JA, Martelli AM (2015) Current treatment strategies for inhibiting mTOR in cancer. *Trends Pharmacol Sci* 36: 124 – 135

Chong-Kopera H, Inoki K, Li Y, Zhu T, Garcia-Gonzalo FR, Rosa JL, Guan KL (2006) TSC1 stabilizes TSC2 by inhibiting the interaction between TSC2 and the HERC1 ubiquitin ligase. *J Biol Chem* 281: 8313 – 8316

Colombetti S, Basso V, Mueller DL, Mondino A (2006) Prolonged TCR/CD28 engagement drives IL-2-independent T cell clonal expansion through signaling mediated by the mammalian target of rapamycin. *J Immunol* 176: 2730 – 2738

Delgoffe GM, Kole TP, Zheng Y, Zarek PE, Matthews KL, Xiao B, Worley PF, Kozma SC, Powell JD (2009) The mTOR kinase differentially regulates effector and regulatory T cell lineage commitment. *Immunity* 30: 832 – 844

Delgoffe GM, Pollizzi KN, Waickman AT, Heikamp E, Meyers DJ, Horton MR, Xiao B, Worley PF, Powell JD (2011) The kinase mTOR regulates the differentiation of helper T cells through the selective activation of signaling by mTORC1 and mTORC2. *Nat Immunol* 124: 295 – 303

Demetriades C, Doumpas N, Teleman AA (2014) Regulation of TORC1 in response to amino acid starvation via lysosomal recruitment of TSC2. *Cell* 156: 786 – 799

Deng L, Qian G, Zhang S, Zheng H, Fan S, Lesinski GB, Owonikoko TK, Ramalingam SS, Sun SY (2019) Inhibition of mTOR complex 1/p70 S6 kinase signaling elevates PD-L1 levels in human cancer cells through enhancing protein stabilization accompanied with enhanced β-TrCP degradation. *Oncogene* 38: 6270 – 6282

Dumont FJ, Staruch MJ, Koprak SL, Melino MR, Sigal NH (1990) Distinct mechanisms of suppression of murine T cell activation by the related macrolides FK-506 and rapamycin. *J Immunol* 144: 251 – 258

Düvel K, Yecies JL, Menon S, Raman P, Lipovsky AI, Souza AL, Triantafellow E, Ma Q, Gorski R, Cleaver S *et al* (2010) Activation of a metabolic gene regulatory network downstream of mTOR complex 1. *Mol Cell* 39: 171 – 183

Farhood B, Najafi M, Mortezaee K (2019) $CD8^+$ cytotoxic T lymphocytes in cancer immunotherapy: a review. *J Cell Physiol* 234: 8509 – 8521

Faul F, Erdfelder E, Lang AG, Buchner A (2007) G*power 3: a flexible statistical power analysis program for the social, behavioral, and biomedical sciences. *Behav Res Methods* 39: 175 – 191

Frias MA, Thoreen CC, Jaffe JD, Schroder W, Sculley T, Carr SA, Sabatini DM (2006) mSin1 is necessary for Akt/PKB phosphorylation, and its isoforms define three distinct mTORC2s. *Curr Biol* 16: 1865 – 1870

Gao J, Shi LZ, Zhao H, Chen J, Xiong L, He Q, Chen T, Roszik J, Bernatchez C, Woodman SE *et al* (2016) Loss of IFN-γ pathway genes in tumor cells as a mechanism of resistance to anti-CTLA-4 therapy. *Cell* 167: 397 – 404

Garami A, Zwartkruis FJT, Nobukuni T, Joaquin M, Roccio M, Stocker H, Kozma SC, Hafen E, Bos JL, Thomas G (2003) Insulin activation of Rheb, a mediator of mTOR/S6K/4E-BP signaling, is inhibited by TSC1 and 2. *Mol Cell* 11: 1457 – 1466

Gerlinger M, Rowan AJ, Horswell S, Math M, Larkin J, Endesfelder D, Gronroos E, Martinez P, Matthews N, Stewart A *et al* (2012) Intratumor heterogeneity and branched evolution revealed by multiregion sequencing. *N Engl J Med* 366: 883 – 892

Gide TN, Quek C, Menzies AM, Tasker AT, Shang P, Holst J, Madore J, Lim SY, Velickovic R, Wongchenko M *et al* (2019) Distinct immune cell populations define response to anti-PD-1 monotherapy and anti-PD-1/anti-CTLA-4 combined therapy. *Cancer Cell* 35: 238 – 255

Gomez-Eerland R, Nuijen B, Heemskerk B, van Rooij N, van den Berg JH, Beijnen JH, Uckert W, Kvistborg P, Schumacher TN, Haanen JBAG *et al* (2014) Manufacture of gene-modified human T-cells with a memory stem/central memory phenotype. *Hum Gene Ther Methods* 25: 277 – 287

Grabiner BC, Nardi V, Birsoy K, Possemato R, Shen K, Sinha S, Jordan A, Beck AH, Sabatini DM (2014) A diverse array of cancer-associated mTOR mutations are hyperactivating and can predict rapamycin sensitivity. *Cancer Discov* 4: 554 – 563

Grolleau A, Bowman J, Pradet-Balade B, Puravs E, Hanash S, Garcia-Sanz JA, Beretta L (2002) Global and specific translational control by rapamycin in T cells uncovered by microarrays and proteomics. *J Biol Chem* 277: 22175 – 22184

Harrington LS, Findlay GM, Gray A, Tolkacheva T, Wigfield S, Rebholz H, Barnett J, Leslie NR, Cheng S, Shepherd PR *et al* (2004) The TSC1-2 tumor suppressor controls insulin-PI3K signaling via regulation of IRS proteins. *J Cell Biol* 166: 213 – 223

He L, Gomes AP, Wang X, Yoon SO, Lee G, Nagiec MJ, Cho S, Chavez A, Islam T, Yu Y *et al* (2018) mTORC1 promotes metabolic reprogramming by the suppression of GSK3-dependent Foxk1 phosphorylation. *Mol Cell* 70: 949 – 960

Hodi FS, O'Day SJ, McDermott DF, Weber RW, Sosman JA, Haanen JB, Gonzalez R, Robert C, Schadendorf D, Hassel JC *et al* (2010) Improved survival with Ipilimumab in patients with metastatic melanoma. *N Engl J Med* 363: 711 – 723

Hosokawa N, Hara T, Kaizuka T, Kishi C, Takamura A, Miura Y, Iemura SI, Natsume T, Takehana K, Yamada N *et al* (2009) Nutrient-dependent mTORC1 association with the ULK1-Atg13-FIP200 complex required for autophagy. *Mol Biol Cell* 20: 1981 – 1991

Hua H, Kong Q, Zhang H, Wang J, Luo T, Jiang Y (2019) Targeting mTOR for cancer therapy. *J Hematol Oncol* 121: 1 – 19

Huang J, Manning BD (2009) A complex interplay between Akt, TSC2, and the two mTOR complexes. *Biochem Soc Trans* 37: 217 – 222

Huang J, Dibble CC, Matsuzaki M, Manning BD (2008) The TSC1-TSC2 complex is required for proper activation of mTOR complex 2. *Mol Cell Biol* 28: 4104 – 4115

Huang Q, Li F, Hu H, Fang Z, Gao Z, Xia G, Ng WL, Khodadadi-Jamayran A, Chen T, Deng J *et al* (2022) Loss of TSC1/TSC2 sensitizes immune checkpoint blockade in non-small cell lung cancer. *Sci Adv* 8: eabi9533

Inoki K, Li Y, Zhu T, Wu J, Guan KL (2002) TSC2 is phosphorylated and inhibited by Akt and suppresses mTOR signalling. *Nat Cell Biol* 4: 648 – 657

Inoki K, Li Y, Xu T, Guan KL (2003a) Rheb GTpase is a direct target of TSC2 GAP activity and regulates mTOR signaling. *Genes Dev* 17: 1829 – 1834

Inoki K, Zhu T, Guan KL (2003b) TSC2 mediates cellular energy response to control cell growth and survival. *Cell* 115: 577 – 590

Inoki K, Ouyang H, Zhu T, Lindvall C, Wang Y, Zhang X, Yang Q, Bennett C, Harada Y, Stankunas K *et al* (2006) TSC2 integrates Wnt and energy signals via a coordinated phosphorylation by AMPK and GSK3 to regulate cell growth. *Cell* 126: 955 – 968

Jiang WG, Sampson J, Martin TA, Lee-Jones L, Watkins G, Douglas-Jones A, Mokbel K, Mansel RE (2005) Tuberin and hamartin are aberrantly expressed and linked to clinical outcome in human breast cancer: the role of promoter methylation of TSC genes. *Eur J Cancer* 41: 1628 – 1636

Jiang P, Gu S, Pan D, Fu J, Sahu A, Hu X, Li Z, Traugh N, Bu X, Li B *et al* (2018) Signatures of T cell dysfunction and exclusion predict cancer immunotherapy response. *Nat Med* 2410: 1550 – 1558

Kakiuchi Y, Yurube T, Kakutani K, Takada T, Ito M, Takeoka Y, Kanda Y, Miyazaki S, Kuroda R, Nishida K (2019) Pharmacological inhibition of mTORC1 but not mTORC2 protects against human disc cellular apoptosis, senescence, and extracellular matrix catabolism through Akt and autophagy induction. *Osteoarthr Cartil* 27: 965 – 976

Kang YJ, Lu MK, Guan KL (2010) The TSC1 and TSC2 tumor suppressors are required for proper ER stress response and protect cells from ER stress-induced apoptosis. *Cell Death Differ* 181: 133 – 144

Kennedy SG, Wagner AJ, Conzen SD, Jordán J, Bellacosa A, Tsichlis PN, Hay N (1997) The PI 3-kinase/Akt signaling pathway delivers an anti-apoptotic signal. *Genes Dev* 11: 701 – 713

Kim DH, Sarbassov DD, Ali SM, King JE, Latek RR, Erdjument-Bromage H, Tempst P, Sabatini DM (2002) mTOR interacts with raptor to form a nutrient-sensitive complex that signals to the cell growth machinery. *Cell* 110: 163 – 175

Kim J, Kundu M, Viollet B, Guan KL (2011) AMPK and mTOR regulate autophagy through direct phosphorylation of Ulk1. *Nat Cell Biol* 13: 132 – 141

Larkin J, Chiarion-Sileni V, Gonzalez R, Grob JJ, Cowey CL, Lao CD, Schadendorf D, Dummer R, Smylie M, Rutkowski P *et al* (2015) Combined Nivolumab and Ipilimumab or monotherapy in untreated melanoma. *N Engl J Med* 373: 23 – 34

Larkin J, Chiarion-Sileni V, Gonzalez R, Grob J-J, Rutkowski P, Lao CD, Cowey CL, Schadendorf D, Wagstaff J, Dummer R *et al* (2019) Five-year survival with combined Nivolumab and Ipilimumab in advanced melanoma. *N Engl J Med* 381: 1535 – 1546

Lastwika KJ, Wilson W, Li QK, Norris J, Xu H, Ghazarian SR, Kitagawa H, Kawabata S, Taube JM, Yao S *et al* (2016) Control of PD-L1 expression by oncogenic activation of the AKT-mTOR pathway in non-small cell lung cancer. *Cancer Res* 76: 227 – 238

Lawson KA, Sousa CM, Zhang X, Kim E, Akthar R, Caumanns JJ, Yao Y, Mikolajewicz N, Ross C, Brown KR *et al* (2020) Functional genomic landscape of cancer-intrinsic evasion of killing by T cells. *Nature* 586: 1 – 7

Li W, Xu H, Xiao T, Cong L, Love MI, Zhang F, Irizarry RA, Liu JS, Brown M, Liu XS (2014) MAGeCK enables robust identification of essential genes from genome-scale CRISPR/Cas9 knockout screens. *Genome Biol* 15: 554

Liberzon A, Birger C, Thorvaldsdóttir H, Ghandi M, Mesirov JP, Tamayo P (2015) The molecular signatures database (MSigDB) hallmark gene set collection. *Cell Syst* 1: 417 – 425

Litchfield K, Reading JL, Puttick C, Thakkar K, Abbosh C, Bentham R, Watkins TBK, Rosenthal R, Biswas D, Rowan A *et al* (2021) Meta-analysis of tumor- and T cell-intrinsic mechanisms of sensitization to checkpoint inhibition. *Cell* 184: 596 – 614

Liu GY, Sabatini DM (2020) mTOR at the nexus of nutrition, growth, ageing and disease. *Nat Rev Mol Cell Biol* 214: 183 – 203

Liu J, Lichtenberg T, Hoadley KA, Poisson LM, Lazar AJ, Cherniack AD, Kovatich AJ, Benz CC, Levine DA, Lee AV *et al* (2018) An integrated TCGA Pan-cancer clinical data resource to drive high-quality survival outcome analytics. *Cell* 173: 400 – 416

Magnuson B, Ekim B, Fingar DC (2012) Regulation and function of ribosomal protein S6 kinase (S6K) within mTOR signalling networks. *Biochem J* 441: 1 – 21

Manning BD, Tee AR, Logsdon MN, Blenis J, Cantley LC (2002) Identification of the tuberous sclerosis complex-2 tumor suppressor gene product tuberin as a target of the phosphoinositide 3-kinase/akt pathway. *Mol Cell* 10: 151 – 162

Martínez-Lostao L, Anel A, Pardo J (2015) How do cytotoxic lymphocytes kill cancer cells? *Clin Cancer Res* 21: 5047 – 5056

Menon S, Manning BD (2009) Common corruption of the mTOR signaling network in human tumors. *Oncogene* 272: S43 – S51

Menon S, Dibble CC, Talbott G, Hoxhaj G, Valvezan AJ, Takahashi H, Cantley LC, Manning BD (2014) Spatial control of the TSC complex integrates insulin and nutrient regulation of mTORC1 at the lysosome. *Cell* 156: 771 – 785

Meyuhas O (2008) Physiological roles of ribosomal protein S6: one of its kind. *Int Rev Cell Mol Biol* 268: 1 – 37

Mills RE, Jameson JM (2009) T cell dependence on mTOR signaling. *Cell Cycle* 8: 545 – 548

Nesterov A, Lu X, Johnson M, Miller GJ, Ivashchenko Y, Kraft AS (2001) Elevated Akt activity protects the prostate cancer cell line LNCaP from TRAIL-induced apoptosis. *J Biol Chem* 276: 10767 – 10774

Ng S, Wu YT, Chen B, Zhou J, Shen HM (2011) Impaired autophagy due to constitutive mTOR activation sensitizes TSC2-null cells to cell death under stress. *Autophagy* 7: 1173 – 1186

Potter CJ, Pedraza LG, Xu T (2002) Akt regulates growth by directly phosphorylating TSC2. *Nat Cell Biol* 4: 658 – 665

Rao RR, Li Q, Odunsi K, Shrikant PA (2010) The mTOR kinase determines effector versus memory $CD8^+$ T cell fate by regulating the expression of transcription factors T-bet and Eomesodermin. *Immunity* 32: 67 – 78

Riaz N, Havel JJ, Makarov V, Desrichard A, Urba WJ, Sims JS, Hodi FS, Martín-Algarra S, Mandal R, Sharfman WH *et al* (2017) Tumor and microenvironment evolution during immunotherapy with Nivolumab. *Cell* 171: 934 – 949

Russell JH, Ley TJ (2002) Lymphocyte-mediated cytotoxicity. *Annu Rev Immunol* 20: 323 – 370

Sato T, Nakashima A, Guo L, Coffman K, Tamanoi F (2010) Single amino-acid changes that confer constitutive activation of mTOR are discovered in human cancer. *Oncogene* 29: 2746 – 2752

Saxton RA, Sabatini DM (2017) mTOR signaling in growth, metabolism, and disease. *Cell* 168: 960 – 976

Schadendorf D, Wolchok JD, Stephen Hodi F, Chiarion-Sileni V, Gonzalez R, Rutkowski P, Grob JJ, Lance Cowey C, Lao CD, Chesney J *et al* (2017) Efficacy and safety outcomes in patients with advanced melanoma who discontinued treatment with Nivolumab and Ipilimumab because of adverse events: a pooled analysis of randomized phase II and III trials. *J Clin Oncol* 35: 3807 – 3814

Schaefer CF, Anthony K, Krupa S, Buchoff J, Day M, Hannay T, Buetow KH (2009) PID: the pathway interaction database. *Nucleic Acids Res* 37: D674 – D679

Shah OJ, Wang Z, Hunter T (2004) Inappropriate activation of the TSC/Rheb/mTOR/S6K cassette induces IRS1/2 depletion, insulin resistance, and cell survival deficiencies. *Curr Biol* 14: 1650 – 1656

Sharma P, Hu-Lieskovan S, Wargo JA, Ribas A (2017) Primary, adaptive, and acquired resistance to cancer immunotherapy. *Cell* 168: 707 – 723

Shi Y, Yan H, Frost P, Gera J, Lichtenstein A (2005) Mammalian target of rapamycin inhibitors activate the AKT kinase in multiple myeloma cells by up-regulating the insulin-like growth factor receptor/insulin receptor substrate-1/phosphatidylinositol 3-kinase cascade. *Mol Cancer Ther* 4: 1533 – 1540

Shin DS, Zaretsky JM, Escuin-Ordinas H, Garcia-Diaz A, Hu-Lieskovan S, Kalbasi A, Grasso CS, Hugo W, Sandoval S, Torrejon DY *et al* (2017) Primary resistance to PD-1 blockade mediated by JAK1/2 mutations. *Cancer Discov* 7: 188 – 201

Sinclair LV, Finlay D, Feijoo C, Cornish GH, Gray A, Ager A, Okkenhaug K, Hagenbeek TJ, Spits H, Cantrell DA (2008) Phosphatidylinositol-3-OH kinase and nutrient-sensing mTOR pathways control T lymphocyte trafficking. *Nat Immunol* 95: 513 – 521

Snajdauf M, Havlova K, Vachtenheim J, Ozaniak A, Lischke R, Bartunkova J, Smrz D, Strizova Z (2021) The TRAIL in the treatment of human cancer: an update on clinical trials. *Front Mol Biosci* 8: 87

Spranger S, Bao R, Gajewski TF (2015) Melanoma-intrinsic β-catenin signalling prevents anti-tumour immunity. *Nature* 523: 231 – 235

Sun SY, Rosenberg LM, Wang X, Zhou Z, Yue P, Fu H, Khuri FR (2005) Activation of Akt and eIF4E survival pathways by rapamycin-mediated mammalian target of rapamycin inhibition. *Cancer Res* 65: 7052 – 7058

Tee AR, Manning BD, Roux PP, Cantley LC, Blenis J (2003) Tuberous sclerosis complex gene products, Tuberin and Hamartin, control mTOR signaling by acting as a GTPase-activating protein complex toward Rheb. *Curr Biol* 13: 1259 – 1268

Thommen DS, Schumacher TN (2018) T cell dysfunction in cancer. *Cancer Cell* 33: 547 – 562

Valvezan AJ, Turner M, Belaid A, Lam HC, Miller SK, McNamara MC, Baglini C, Housden BE, Perrimon N, Kwiatkowski DJ *et al* (2017) mTORC1 couples nucleotide synthesis to nucleotide demand resulting in a targetable metabolic vulnerability. *Cancer Cell* 32: 624 – 638

Vredevoogd DW, Apriamashvili G, Peeper DS (2021) The (re)discovery of tumor-intrinsic determinants of immune sensitivity by functional genetic screens. *Immunooncol Technol* 11: 100043. https://doi.org/10.1016/j.iotech.2021.100043

Vredevoogd DW, Kuilman T, Ligtenberg MA, Boshuizen J, Stecker KE, de Bruijn B, Krijgsman O, Huang X, Kenski JCN, Lacroix R *et al* (2019) Augmenting immunotherapy impact by lowering tumor TNF cytotoxicity threshold. *Cell* 178: 585 – 599

Wang S, El-Deiry WS (2003) TRAIL and apoptosis induction by TNF-family death receptors. *Oncogene* 22: 8628 – 8633

Wang Y, Hu Z, Liu Z, Chen R, Peng H, Guo J, Chen X, Zhang H (2013) MTOR inhibition attenuates DNA damage and apoptosis through autophagy-mediated suppression of CREB1. *Autophagy* 9: 2069 – 2086

Wherry EJ, Kurachi M (2015) Molecular and cellular insights into T cell exhaustion. *Nat Rev Immunol* 158: 486 – 499

Wolchok JD, Chiarion-Sileni V, Gonzalez R, Rutkowski P, Grob J-J, Cowey CL, Lao CD, Wagstaff J, Schadendorf D, Ferrucci PF *et al* (2017) Overall survival

with combined Nivolumab and Ipilimumab in advanced melanoma. *N Engl J Med* 377: 1345 – 1356

Xu Z, Wang M, Wang L, Wang Y, Zhao X, Rao Q, Wang J (2009) Aberrant expression of TSC2 gene in the newly diagnosed acute leukemia. *Leuk Res* 33: 891 – 897

Young L, Sung J, Masters JR (2010) Detection of mycoplasma in cell cultures. *Nat Protoc* 5: 929 – 934

Zaretsky JM, Garcia-Diaz A, Shin DS, Escuin-Ordinas H, Hugo W, Hu-Lieskovan S, Torrejon DY, Abril-Rodriguez G, Sandoval S, Barthly L *et al* (2016) Mutations associated with acquired resistance to PD-1 blockade in melanoma. *N Engl J Med* 375: 819 – 829

Zarour HM (2016) Reversing T-cell dysfunction and exhaustion in cancer. *Clin Cancer Res* 22: 1856 – 1864

Zhang Y, Gao X, Saucedo LJ, Ru B, Edgar BA, Pan D (2003) Rheb is a direct target of the tuberous sclerosis tumour suppressor proteins. *Nat Cell Biol* 5: 578 – 581

Zhang Z, Kong X, Ligtenberg MA, van Hal-van Veen SE, Visser NL, de Bruijn B, Stecker K, van der Helm PW, Kuilman T, Hoefsmit EP *et al* (2022) RNF31 inhibition sensitizes tumors to bystander killing by innate and adaptive immune cells. *Cell Rep Med* 3: 100655. https://doi.org/10.1016/j.xcrm.2022.100655

Zheng Y, Collins SL, Lutz MA, Allen AN, Kole TP, Zarek PE, Powell JD (2007) A role for mammalian target of rapamycin in regulating T cell activation versus Anergy. *J Immunol* 178: 2163 – 2170

Zimmerer RM, Korn P, Demougin P, Kampmann A, Kokemüller H, Eckardt AM, Gellrich NC, Tavassol F (2013) Functional features of cancer stem cells in melanoma cell lines. *Cancer Cell Int* 13: 1 – 13